2018

Hotspot characterization and detonation initiation in thermally stratified reactive mixtures

Fynn Reinbacher
Iowa State University

Hotspot characterization and detonation initiation

in thermally stratified reactive mixtures

by

Fynn Reinbacher

A thesis submitted to the graduate faculty

in partial fulfillment of the requirements for the degree of

MASTER OF SCIENCE

Major: Aerospace Engineering

Program of Study Committee:
Thomas Ward III, Major Professor
Jonathan D. Regele
James B. Michael

The student author, whose presentation of the scholarship herein was approved by the program of study committee, is solely responsible for the content of this thesis. The Graduate College will ensure this thesis is globally accessible and will not permit alterations after a degree is conferred.

Iowa State University

Ames, Iowa

2018

DEDICATION

To my parents,

my siblings,

and my friends,

both at home and abroad.

TABLE OF CONTENTS

Page

LIST OF TABLES

Page

LIST OF FIGURES

Page

ACKNOWLEDGMENTS

I would like to express my gratitude to all those who helped and supported me throughout my studies, helped me while conducting my research and finally writing this thesis.

First and foremost, to Dr. Jonathan D. Regele under whose guidance I started my journey at Iowa State for his constant support and advice throughout my research.

Further I would like to thank the other members of my committee, my major professor Dr. Thomas Ward and Dr. James B. Michael for their ideas and advise.

I thank all my colleagues at Iowa State University for many fruitful discussion, ideas, advice, encouragement, support and friendship, especially my research group: Mohamad Aslani, Wyatt Hagen, Michael Phillips, Dan Garrick, and Zahra Hosseinzadeh-Nik.

Finally I would like to thank all my friends and family who have made me feel at home no matter where between two continents I was, at every step along my journey.

ABSTRACT - ENGLISH

In a society powered by combustion, a detailed understanding of the underlying physics is imperative. Among the main challenges in the development of high performance, high efficiency advanced gasoline engines are end-gas, auto- or pre-ignition and super-knock, a phenomenon attributed to the formation of detonation waves. Detonations, while wanted in few select applications, are generally to be avoided in any combustion system due to the attributed high over pressures. Hotspots, regions of higher temperature or reactivity, play a key role in understanding both autoignition and detonation initiation. Critical factors determining the thermomechanical response of a fluid to a local hotspot strongly depend on the hotspot size, temperature and temperature in the surrounding fluid, all of which influence different timescales of the ignition process. As such common modeling approaches for hotspots include rapid spatially resolved energy deposition or energy deposition through boundaries, and modeling via spatially resolved thermal stratification, such as linear temperature gradients or sinusoids. This thesis aims to improve hotspot modeling methods, by introducing a method to model a wide range of smooth temperature distributions with a small amount of parameters, and by introducing a new characterization method for the critical timescales during the initial hotspot ignition process.

First a new modeling approach is introduced in order to investigate the influence of smooth temperature variations on hotspot ignition. Previous studies have already shown that temperature plateaus, modeling a hotspot center of finite size, can facilitate detonations in temperature gradients that otherwise wouldn't. Realistic temperature distributions however, will have some kind of smooth, continuous temperature distribution. A superelliptic model is introduced. Adding only 2 additional parameters compared to the plateau and gradient model, allows this new model to parametrize smooth temperature variations across wide ranges of hotspot core sizes and gradients. Various degrees of smoothness in the curved temperature profile can by achieved by varying a su-

perelliptic exponent. By using an acoustic timescale characterization approach the results obtained could be contrasted with those obtained in previous works. It could be shown that while the intensity of the incidental pressure wave emitted at the reaction of the hotspot center is similar for plateau like and smooth temperature variations. Smooth temperature profiles on the other hand were shown to facilitate much more severe gasdynamic responses than discontinuous temperature distributions. It was further shown that hotspots considered partially inertially confined by means of an acoustic timescale characterization, can be extremely sensitive to slight variations in the superelliptic exponent and lead to direct detonation initiation.

Second in order to improve the predictability of the pressure response from a local reaction hotspot, a new timescale characterization approach based on critical hotspot expansion timescales is introduced and contrasted to a well investigated acoustic timescale characterization approach. Specifically, this new approach seeks to account for the influence of the fluid surrounding a hotspot on its inertial confinement. The new approach was shown to give a more consistent measure of whether heat release inside a hotspot or fuelpocket will occur isochorically, isobarically or in mix-fashion, and thus whether they will emit weak acoustic, strong compression or blast waves. Over a large temperature range inside the hotspot and in surrounding fluid, hotspots with timescale ratios an order of magnitude smaller than unity would result in a pressure increase equivalent to approximately $90\% \pm 5\%$ of the normalized isochoric pressure increase, while timescales ratios on the order of unity would result in $50\% \pm 10\%$ and ratios much larger than unity around $10\% \pm 5\%$ of the normalized isochoric pressure increase.

ABSTRACT - GERMAN

In einer Gesellschaft angetrieben durch Verbrennungskraft ist ein detailliertes Verständnis der ihr zugrundeliegenden physikalischen Prozessen unabdinglich. Unter den grössten Herausforderungen in der Entwicklung von hochleistungs, hoch-effizienten fortschrittlichen Verbrennungsmotoren sind vorzeitige und Selbstentzündung des Endgases und das damit zusammenhänge Motorklopfen, ein Phänomen welches der Formation von Detonationswellen zugeschrieben werden kann. Detonationen, wenngleich in wenigen ausgewählten Applikationen erwünscht, sind generell zu vermeiden wegen der mit ihnen verbundenen, hohen Druckspitzen. Hotspots, Regionen mit erhöhter Temperatur oder Reaktivität, spielen eine zentrale Rolle im Verständnis von sowohl Selbstentzündung als auch der Initiation von Detonationen. Kritische Faktoren welche die thermomechanische Antwort eines Fluids auf einen lokalen Hotspot bestimmen hängen von der Hotspot Grösse und Temperatur sowie der Temperatur im umliegenden Fluid ab. All diese Faktoren beinflussen dabei insbesondere die für den Entzündungsprozess relevanten Zeitskalen. Viele Modellierungsansätze für Hotspots involvieren daher unteranderem rapide räumlich Deponierung von Energie, Einleitung von Energie über die Systemgrenzen, oder basieren auf der Struktur der räumlichen Temperaturverteilung wie zum Beispiel in linearen Gradienten oder Sinuskurven. Ziel dieser Arbeit ist es Hotspot Modellierungsansätze zu verbessern. Vorgestellt werden eine neue Methode zur Modellierung einer weiten Brandbreite stetiger Temperaturverteilungen mit Hilfe einer möglichst geringen Parameteranzahl, sowie eine Charakterisierungsmethode für die kritischen Zeitskalen während der Hotspotentündung.

Zuerst wird eine neuer Modellierungsantz vorgestellt um den Einfluss stetiger Variationen in der Hotspot Temperaturverteilung auf den Entzündungsvorgang zu untersuchen. Frühere Studien haben bereits gezeigt, das Temperaturplateaus, welche ein Hotspotzentrum von finiter Grösse repräsentiert, eine Detonationswelle in umliegenden Temperaturgradienten erzeugen können, welche ohne anschliessendem Temperaturplateau dazu nicht in der Lage wären. Realistische Temper-

aturfelder wiederum zeichnen sich durch kontinuierlich, stetige Temperaturverteilungen aus. Ein superelliptisches Modell wird daher vorgestellt. Mit Hilfe von 2 zusätzliche Parametern die dem Plateau und Gradienten model hinzugefügt werden wird es dem neuen Modell möglich stedige Temperaturfelder über eine weite Bandbreite von Hotspot Kerngrössen und Gradienten zu modellieren. Verschiedene Krümmungsgrade im Temperaturprofil können dabei über Variation eines superelliptischen Exponentens erzeugt werden. Mit Hilfe eines Charakterisierungsverfahrens basierend auf akustischen Zeitskalen, ist desweiteren möglich die Ergebnisse mit denen vorheriger Studien zu vergleichen. Es konnte gezeigt werden, dass die Intensität der Druckwelle ausgesandt mit Beginn der Reaktion im Hotspotzentrum, ähnlich für sowohl Plateau und Gradienten als auch kontinuierliche Temperaturfelder ist. Kontinuirliche Temperaturfelder können allerdings im Gegensatz zu diskontinuierlichen Temperaturfelder zu weitaus schwerwiegenderen gasdynamischen Reaktionen führen. Desweiteren konnte gezeigt werden, dass Hotspots welche basierend auf der Charakterisierung mit Hilfe akustischer Zeitskalen teilweisem Trägheitseinschluss unterliegen, besonders empfindlich gegenüber Veränderungen im superelliptischen Exponenten sind und so zur direkten Initiation von Detonationen führen können.

Zweitens wird eine neue Charakterisierung von Hotspots basierend auf kritischen Expansionszeitskalen vorgestellt und mit der bereits weitreichend untersuchten Charakterisierung mittels akustischer Zeitskalen verglichen, um die Genauigkeit über die Druckentwicklung während der lokalen Reaktion eines Hotspots zu verbessern. Insbesondere wird mittels dieser Methode versucht den Einfluss der Temperatur des den Hotspots umgebenden Fluids auf dessen Trägheitseinschluss zu berücksichtigen. Diese neue Methode zeichnete sich durch ein einheitlicheres Maß dafür aus, ob ein Hotspot isochor, isobar oder gemischt isobar und isochor reagiert, und somit ob schwache akustische, starke Kompressions- oder Stoßwellen erzeugt werden. Über eine weite Bandbreite von Temperaturen im Hotspot und dem umgebenden Fluid zeigten Hotspots mit einem Zeitskalenverhältnis deutlich kleiner als Eins einen Druckanstieg um $90\% \pm 5\%$ des normalisierten isochorischen Druckanstiegs, während solche mit einem Zeitskalenverhältnis in der Grössenordnung von

Eins einen Anstieg um $50\% \pm 10\%$ und solche mit Verhältnissen deutlich grösser als Eins einen Anstieg um $10\% \pm 5\%$ des normalisierten isochorischen Druckanstieges erreichten.

CHAPTER 1. OVERVIEW

1.1 Introduction

Combustion processes in today's world are ubiquitous, from candle light to forest fires, internal combustion engines to power plants, and fire crackers to mining accidents. Whether the combustion itself is desired or not, each flame needs to ignited first. The ignition itself in many cases can have a significant influence on the rate of the consecutive reaction. Ignition can be caused in various fashions: by a spark, an electric discharge, frictional heating, photo-chemically by laser or other light sources, or by autoignition in a thermally stratified field. No matter which method is used the underlying mechanism remains the same. An amount of energy is deposited locally, which causes sufficient heat to be released by a combustible mixture, to cause self-sustained reaction in the surrounding mixture. These local pockets of with increased reactivity can also be referred to as a hotspots and they can play a crucial role in understanding the physics of a combustion problem.

While often in many systems reactions occur at constant pressure, if reactions become rapid enough this is no longer necessarily the case. Large enough pressure perturbations in turn can influence and accelerate the chemical reaction. A strong pressure wave traveling at supersonic speeds, also called a shock wave, sustained by the heat release from a coupled chemical reaction in a combustible mixture, is also called a detonation. While there are few select applications, including but not limited to Pulsed and Rotational Detonation Engines (PDE, RDE) or explosives in mining or demolition applications, in which generating a detonation may be desirable and the release energy harnessed for beneficial purposes, generally they are sought to be avoided, due to their destructive nature. Understanding under which conditions detonation waves can form and initiated is therefore crucial to avoid potential hazards.

It is easy to imagine how an ignition kernel can potentially directly initiate a detonation wave. Hotspots may however also form in accelerating flame fronts and facilitate a transition from a slow

deflagration to detonation (DDT) under certain conditions, a phenomenon to which Oppenheim [41] refers to as "an explosion in the explosion". Understanding the gasdynamic response of a reactive medium to the autoignition of a hotspot aide in analyzing DDT processes, detonation initiation and ignition in general. This thesis therefore focuses on the characterization and modeling of hotspot ignition. Specifically the influences of the temperature distribution within a hotspot on its ignition behavior and the characteristic timescales are emphasized. More detailed background on the current state of research on autoignition, hotspots, characteristic timescales involved and the detonation phenomenon are given in the subsequent section.

1.2 Background

1.2.1 Detonation

The term detonation originally derives form the latin word detonare, meaning 'to thunder down'. Research involving its modern use for describing shock wave driven by a supersonic combustion wave roughly dates back to the beginning of the 20th century. Most notable are probably the works of David Chapman in 1899 [7] and Emile Jouguet [20], who were search of an algebraic description of observations found in the works of Mallard and Le Chatelier, Berthelot and Vielle, who -as Jouguet puts it- "made a breakthrough discovery, even more beautiful than that of chemical mechanisms, of a phenomenon of an explosive wave, in which a reaction propagates in a gaseous medium with a regular velocity of several thousand meters per second". Based on the theories on wave propagation by Rankine, Riemann and Hugoniot they derived the conditions for an infinitesimally thin detonation wave propagating at supersonic speeds.

With the increasing demand for high-powered explosives during world-war II and the race towards the development of a thermonuclear weapon Soviet scientist Yakov Zel'dovich, Hungarian-American scientist John von Neumann, and German scientist Werner Döring each developed a one-dimensional model for a detonation [72, 66, 15]. The ZND detonation model which was named after them, describes a one-dimensional steady detonation wave. It is composed of a shock-wave followed by a reaction zone. In the reference frame of the shock, the flow at the of the reaction

zone is locally sonic and all fuel is consumed. This way all energy released by the chemical reaction behind the shock gets acoustically transported upstream and the shock can be supported. The Chapman-Jouguet (CJ) condition gives the shock speed necessary to form this stable structure.

As important as it is to understand the structure of detonations is, is understanding the pathways through which they can develop. Generally detonations can either by initiated directly or develop from intrinsically unstable deflagrations [33] through deflagration to detonation transition (DDT). There is not one unique way to initiate a detonation or for a DDT to take place as described by Urtiew and Oppenheim [63]. In an accelerating flame brush precursor shock was form which and merge, causing subsequent autoignition. Local hotspots can cause additional blast waves from an explosion in an explosion. Transverse pressure waves reflect off the tube walls amplifying the pressure in the reaction front.

Similarly direct initiation can be achieved by various means and mechanisms. In contrast to DDT where favourable conditions to facilitate detonation form over time, the ignition source itself is responsible for preconditioning the flow field and facilitating the detonation formation [33]. Direct initiation methods are especially interesting for the formation of spherical detonations. Unlike planar detonations, steady cylindrical or spherical CJ-detonations can't exist due to the lack of confinement [71]. Means of initiation generally involve the induction of chemical breakdown, the generation of a blast wave or rapid heating through explosive charges, wires, spark gaps, lasers or high velocity jets [3, 16, 75, 57].

Many factors can influence the ignition and detonation initiation process. For the ignition itself the driving factor the minimum ignition energy plays a critical role [69]. Similarly for a for autoignition to occur in a hotspot and subsequently aide in transition to detonation, the temperature in the local hotspot needs to be high enough for the auto-ignition energy to approach zero. Just depositing the minimum ignition energy however is not necessarily sufficient if depending on local energy transport processes involved. For direct initiation of gaseous detonations Knystautas and Lee for example have shown already in 1976 that the critical amount of energy is not necessarily unique, but depends on the rate of deposition [30]. If energy is deposited via a spark, any en-

ergy deposited past the time of peak averaged power, has no influence on the detonation initiation process.

What all pathways to detonation onset have in common, is that they involve the formation of conditions under which the interaction and timing between heat release and pressure waves synchronizes and amplifies. Zeldovich et al. [74] showed in 1970 that detonations can form along a spatial gradient of the ignition delay time in a combustible mixture. Since the ignition delay mostly dependent on the temperature, this translates essentially into the formation of a detonation along a linear temperature gradient. Later Lee et al [34] were able to further expand upon this idea of detonation initiation via the correct timing between chemical heat release and shock wave in their photo-initiation experiments. They called their discovered gradient mechanism SWACER or Shock Wave Amplification by Coherent Energy release.

1.2.2 Hotspots

1.2.2.1 Hotspots in Combustion Systems

A hotspot describes a small region within a reactive medium, which is distinguished form its surroundings by a higher temperature or reactivity. The generation and presence of hotspots can be traced back to various mechanisms ranging from mechanical friction to localized exothermic reactions or pressure fluctuations [58, 42, 28]. As Sankaran et al. have shown [54, 8] the combustion in a thermally stratified mixture may occur either in flame like or volumetric fashion leading to the generation of either weak acoustic waves or stronger compression waves. Further investigation of the ignition kernels in the inhomogenous temperature field and the hazards these hotspots pose is of interest.

Spatially distributed temperature fields incorporating numerous hotspots can often be found for example in internal combustion engines such as HCCI engines. Here autoignition is responsible for effects such as super-knock [22, 6]. Here the spatial temperature variations develop mostly close to the walls and evolve from small, evenly distributed greater fluctuations during the compression stroke which later convect towards the center, as shown by a laser-induced fluorescence measurement

on an optically accessible engine by Kaiser et al. [21]. Similar results were obtained by Schmitt et al. in an investigation of the wall heat transfer during DNS simulations of intake and compression stroke under engine relevant conditions. Large vortical structures which evolve during the intake at the valves promoted heat transfer from the walls towards the center. Overall mixing is strongly influenced by turbulence and break down of large structures during the compression stroke [56, 55].

As hotspots and DDT have long been suspected as sources of super-knock in internal combustion engines, it has not been directly observed until 2014 by Wang et al. [67]. In a optically accessible rapid compression machine fueled with an iso-octane-air mixture they observed various modes of knock, due to endgas autoignition and hot-spot induced detonation. The latter resulted in over-pressures of up to 4 times the regular cycle pressures at unfavorable crank-angles. More recently Mubarak et al. [18] used computer simulations to study the impact of timing and location of the hotspot on the knock intensity.

As mentioned before turbulent mixing has a significant influence on the the formation of thermal stratification in combustion engines. Chi et al. used Direct Numerical Simulations (DNS) to determine the influence of turbulence intensity on hotspot ignition in an H_2-air mixture [9]. Ignition probability and delay time are found to be mainly dependent on initial hotspot size, temperature and ignition intensity. They further discuss some of the influences of additional dimensionality of the hotspot ignition by including 0D, 1D, 2D and 3D results. They also found that ignition kernels with a critical minimal initial size and temperature lead to ignition without failure.

1.2.2.2 Hotspot Modeling

Due to their importance in detonation initiation and autoignition hotspots have been investigated since the 1960's, in order to stake out critical conditions for different combustion phenomena. The main focus of these studies usually were critical hotspot sizes and temperatures. Different theories on hotspot criticality include such as those of Merzhanov [39] and Thomas [62]. Zaturska [70] further used these approaches based on thermal explosion theory to determine the effect of the interaction between two identical hotspots in proximity to each other. Under the conditions

investigated however no alterations to the reaction behavior of the individual hotspots was observed except for cases of very small separation. In a more recent and detailed study on the interaction between multiple hotspots by Wei et al. [68] found a wider range of pressure responses. The maximum pressure peak and location depends on amplitude, spacing and initial temperature in the undisturbed temperature field. Using Arrhenius kinetics, Clarke [11] and Nikiforakis and Clarke [40] further investigated the evolution of hotspots in flame front and a description of how they evolve into detonations through compression waves emitted during their reaction.

Also using Arrhenius kinetics, wall-type and internal hotspots were investigated by Jackson, Kapila and Steward [19]. In their assumptions they state that under the conditions that reaction and acoustic timescales are short enough compared to diffusion they stated that the same treatment of hotspots holds for both gas and condensed phase explosives. Under these conditions they assume that gasdynamic effects secondary neglecting any potential expansion of the gas, forcing the reaction to occur isochorically.

While the aforementioned hotspot models mostly focus on a description of hotspots as static thermal hotspot, many other paper focused on hotspots in terms of regions of high local heat release or energy deposition. As Sileem, Kassoy and Hayashi [60] and Kassoy et al [26] simulated hotspots by spatially resolved thermal power deposition on an acoustic timescale. The driving mechanism both studies again stems from compression waves generated by the initial energy deposition in the hotspot, preheating the surrounding fluid leading to subsequent heat release. While the initial efforts focused on systems with low activation energies, they were later extended to high activation energies and two dimensions by Regele et al. [46, 47, 52]. High activation energies, as found in more most real world combustion systems, were shown to result in a more temporally distributed heat release. The change in behavior could be characterized using an acoustic timescale ratio. Further it was shown that depending on the timescale ratio either acoustic, shock or blast waves were emitted from the hotspot reaction. In 2 dimensions similar observations as in 1D simulations could be made. Most recently Regele et al. [51] were also able to show that for energy deposited into a fluid volume on an acoustic timescale similar behavior for direct detonation initiation and

DDT can be observed. Further it was shown that the investigated detonation initiation process under the conditions at hand were essentially independent from viscous and diffusive effects.

Along the lines of the works of Zeldovich et al. and Lee et al. [74, 34] in section 1.2.1 other studies focus on the modeling of hotspots in terms of linear temperature gradients. Zeldovich identified 5 different reaction front propagation modes in nonuniform initial conditions [73], which Gu, Emerson and Bradley were later able to identify in in reaction front generated from a hotspot [17]. Kapila et al. [23] found that shallow gradients allow the formation of detonations, while steep gradients don't. Sharpe and Shorte [59] and Liberman et al. [37] further found that including detailed kinetics increased the minimum required gradient length to allow for detonation formation. Kurtz and Regele [31, 32] investigated more realistic hotspot temperature profiles, by including a hotspot center of finite size in shape of an isothermal plateau. Plateaus of sufficient size were shown to induce DDT in gradient which on their own would not.

1.2.3 Acoustic Timescale Characterization

One of the common findings of the studies of hotspot ignition, autoignition and detonation initiation processes is that the relative timescales of energy deposition, energy transport and fluid motion play a significant role in determining the overall gasdynamic behavior. Information about changes of the thermodynamic state within a gas is transported at the local speed of sound, a. The acoustic time t_a can then be described as the time it takes for an acoustic wave to transport information along across some characteristic length scale l. As such the acoustic time gives an indication of the time required for fluid motion to be induced within a fluid volume and thus time required for a fluid to react to changes in density or pressure.

What has been shown in many hotspot studies by experience, that detonation initiation largely depends on the amount of energy locally deposited or rate at which it is deposited, has been formally investigated over the course of many studies [60, 44, 12, 13, 14]. Clarke, Kassoy and others have shown that the pressure response is of a gas depends highly on the rate of energy deposition into

the fluid. Using asymptotic analysis procedure they were able to find equations describing the response of the gas in different phases following the heat addition.

In an full asymptotic analysis of the Navier-Stokes equations on an acoustic timescale, Kassoy [24] parametrizes the reaction of an inert fluid to local heat addition. If heat addition is small during an acoustic heating time period, acoustic waves propagate into the surroundings, while shock waves are produced when heating is large. He later extends this approach to the transient heat addition in a reactive gas [25], where similarly the responses range from weak acoustic waves to strong blast waves.

Regele [49] further applied this characterization on an acoustic timescale to unreacted fuel pockets surrounded by burned reaction products and was able to show that this method allows to distinguish between pockets reacting at nearly constant pressure, constant volume, and any conditions between these two extremes. He further extends these efforts later on to predict the magnitude of the pressure response of reacting fuel pockets created in turbulent reaction fronts and their impact on unsteady detonations [50].

1.3 Objectives and Organization

Hotspot ignition behavior and detonation initiation are often studied in terms of either linear temperature gradient [17, 23] or modeled simple sinusoidal temperature perturbations [68]. In reality however hotspots rarely take such idealized shapes, due to the complex various mechanisms that lead to their formations [54, 8]. Hotspots in thermally stratified fields generally take some curved shape with a local maximum, the hotspot core, surrounded by a gradient region, the hotspot body, in which the temperature either drops of to some ambient condition or into a neighboring cold pocket. Recent efforts sought to investigate the influence of the hotspot core on the reaction of the surrounding hotspot body, by modeling the local maximum at the hotspot center as an isothermal plateau [31, 32]. Using an acoustic timescale characterization approach of the hotspot plateau an a-priori prediction of the gas dynamic response could be made. This work aims to expand on these affords by further investigating the influence of smooth temperature variations between the

hotspot core and body, and further expanding on the acoustic timescale characterization approach by identifying critical timescales of the hotspot ignition process.

The first objective of this work is to provide a more realistic model of the hotspot temperature distribution, that incorporates smooth temperature variations. In an extension of the plateau and gradient approach taken by Kurtz and Regele [31, 32], a superelliptic model is proposed. Hotspots of various sizes are studied and results to show the influence of a smooth temperature variation connecting plateau and gradient regions on the detonation transition behavior. Further the model provides a way to capture the limiting behaviors demarcated by linear temperature gradients and gradients with plateaus on their own.

The second objective is to improve the understanding of the dominant timescales controlling the pressure response during the hotspot ignition. In particular identifying the dominant timescales controlling the hotspot expansion in dependence of the temperature both inside the hotspot and in the surrounding fluid, and comparing the results to those obtained by the previously discussed acoustic timescale characterization methods. The pressure response in dependence of the critical expansion timescale variations is tested for both hotspots in reactive fluids and unreacted fuel pockets.

This thesis contains two papers, one published at the time of this thesis was composed, the other submitted for publication and under review. Chapter 2.8 and 3.7 each contain the entirety of each publication with their own introduction, descriptions of mathematical model, numerical methods, analysis, problem statement, results, discussion and conclusion. A general discussion and conclusion, as well as prospective future work will be featured in chapter 4, followed by a bibliography for the entire thesis.

CHAPTER 2. INFLUENCE OF SMOOTH TEMPERATURE VARIATION ON HOTSPOT IGNITION

A paper published in *Combustion Theory and Modelling* [1]

Fynn Reinbacher [2], Jonathan D. Regele [3,4]

2.1 Abstract

Autoignition in thermally stratified reactive mixtures originates in localized hotspots. The ignition behavior is often characterized using linear temperature gradients and more recently constant temperature plateaus combined with temperature gradients. Acoustic timescale characterization of plateau regions has been successfully used to characterize the type of mechanical disturbance that will be created from a plateau core ignition. This work combines linear temperature gradients with superelliptic cores in order to more accurately account for a local temperature maximum of finite size and the smooth temperature variation contained inside of realistic hotspot centers. A one-step Arrehnius reaction is used to model a H2 air reactive mixture. Using the superelliptic approach a range of behaviors for temperature distributions are investigated by varying the temperature profile between the gradient only and plateau and gradient bounding cases. Each superelliptic case is compared to a respective plateau and gradient case where simple acoustic timescale characterization may be performed. It is shown that hot spots equivalent with excitation-to-acoustic timescale ratios sufficiently greater than unity exhibit behavior very similar to a simple plateau-gradient model. However, for larger hot spots with timescale ratios sufficiently less than unity the reaction behavior is highly dependent on the smooth temperature profile contained within the core region.

[1] *Fynn Reinbacher, Jonathan D. Regele. Influence of smooth temperature variation on hotspot ignition.* Combustion Theory and Modelling V ***22****, (2017)*

[2] Iowa State University Department of Aerospace Engineering

[3] Los Alamos National Laboratory

[4] Author for correspondence: jregele@lanl.gov

2.2 Introduction

Hot spot auto-ignition is a common problem in internal combustion (IC) engines and is responsible for problems like engine knock and pre-ignition. As its name suggests, a hotspot can generally be described as a smaller region within a reactivemixture that is distinguished from its surroundings by a higher temperature or reactivity. The generation and presence of hotspots can be traced back to various mechanisms ranging from mechanical friction to localised exothermic reactions or pressure fluctuations [58, 42, 28]. As Sankaran et al. [54, 8] have shown the combustion in a thermally stratified mixture may occur either in a flame-like or volumetric fashion, leading to the generation of either weak acoustic waves or stronger compression waves. They studied non-uniform initial distributions of temperature and fuel composition in the context of homogeneous charge compression ignition (HCCI) engines. HCCI combustion is dependent on hotspot autoignition. The hotspots form from turbulence and wall heat transfer during compression [56, 55], which can lead to cycle-to-cycle variations of the ignition delay time and high pressure peaks [2, 10].

It is common for hotspots to be described by critical gradient conditions. An abundance of literature exists that analyses the transition and initial conditions that lead to the generation of detonations [39, 62, 74, 35, 36, 34]. Clarke and Nikiforakis [40] and Clarke [11] also show that hotspots can create compression waves, which can cause detonation formation. The evolution of wall-type hotspots, with a temperature gradient at the centre, and internal-type hot spots, with a rounded peak at the centre, are investigated by Jackson, Kapila and Stewart [19]. Gasdynamic effects are treated as secondary in a regime dominated by chemical heating, resulting in constant volume explosions in either case.

The acoustic time, t_a, is the time it takes for an acoustic wave to propagate some characteristic length, l, through a mixture at the local speed of sound, a. If energy is added to a mixture at a timescale much smaller, greater or equal to the acoustic timescale, the fluid will respectively remain inertially confined, expand or remain just partially confined during the reaction. Many papers [43, 44, 12, 13, 22, 6, 17] explored the deposition of energy on different length and timescales and have shown that the gasdynamic response can be characterised by the time duration in which a

sufficient amount of energy is deposited. Regele et al. [47, 52] also investigated the transition from deflagration to detonation for an energy deposition on an acoustic timescale and later extended the 1D model to two dimensions and observed similarities to the one-dimensional model for the deposition of a sufficient amount of energy.

Kassoy [24] performed an asymptotic analysis of the NavierStokes equations and uses the ratio of the heating time to acoustic time to characterise the thermomechanical response of the gas. If heat is added over time longer than the acoustic time, only weak acoustic waves are generated. Additionally, if the heat addition is a lot larger throughout the same period of time shock waves will be sent out. In hotspots characterised by their thermal stratification, heat is released throughout the reaction. Reaction time scales can be related to the acoustic time, similarly to the heating time.

Real hotspots usually take the form of some curve with a local maximum at the centre of a hot core region. Recent studies by Kurtz and Regele [31, 32] attempt to take this into account by studying the influence of a temperature plateau on an adjacent gradient region. It is shown that plateaus of sufficient size facilitate deflagration-to-detonation transition in gradients that would otherwise only create strong compression or shock waves. The inertial confinement of the hotspot core is characterised using the excitation-to-acoustic timescale ratio.With this approach, a priori predictions about hotspot reaction behaviour are made.

While the plateau and gradient model [31, 32] is a first step towards understanding the impact of a hot core region on a surrounding temperature gradient, more realistic models must also incorporate smooth temperature variations within the hot core region. The main objective of this work is to investigate how the reaction of a finite sized hot spot core region with a smooth temperature profile connecting the plateau and gradient regions impacts the detonation transition behaviour. In order to do this, a superelliptic model is proposed that builds on the original plateau and gradient conditions analysed in Kurtz and Regele [31, 32] in order to determine the difference in behaviour. This approach provides a way to model the smooth temperature variations inside the hotspot core

region while simultaneously providing a way to capture the limiting behaviours demarcated by linear temperature gradients and gradients with plateaus.

This paper is structured as follows. First the mathematical model used to simulate the hotspot reaction and thermomechanical response is described in Section 2.3. Timescales governing the fluid behaviour are described in Section 2.4, followed by a formulation of the problem set-up in Section 2.5. In Section 2.6 the numerical methods used to perform the simulations are presented. Finally, in Section 2.7.2, the results are presented and conclusions are drawn in Section 2.8.

2.3 Mathematical Model

The general governing equations for the flow are given by the reactive NavierStokes equations. However, the primary focus of the current work lies on spontaneous waves and autoignition that occur on timescales much shorter than those associated with diffusional processes. In this context the transport effects may be neglected. Justification for this approach is presented in Section 2.4. Furthermore, since the objective is the qualitative characterisation of the fluids thermomechanical response, one-step kinetics are employed, rather than detailed chemistry which would be necessary for quantitative predictions of critical conditions for detonation formation [22, 6, 59, 37]. Therefore, the reactive 1-D Euler equations with a one-step Arrhenius reaction are used. In conservative vector form these are:

$$\frac{\partial \boldsymbol{U}}{\partial t} + \frac{\partial \boldsymbol{F_x}(\boldsymbol{U})}{\partial x} = \boldsymbol{S} \tag{2.1}$$

where:

$$\boldsymbol{U} = \begin{Bmatrix} \rho \\ \rho u \\ \rho e_T \\ \rho Y \end{Bmatrix}, \boldsymbol{F_x} = \begin{Bmatrix} \rho u \\ \rho u^2 + p \\ (\rho e_T + p)u \\ \rho Y u \end{Bmatrix}, \boldsymbol{S} = \begin{Bmatrix} 0 \\ 0 \\ 0 \\ -\dot{W} \end{Bmatrix}. \tag{2.2}$$

Here ρ is the density, ρu is the momentum, e_T is the total energy per unit mass, and Y is the fuel mass fraction. The sum of internal, kinetic and chemical energy yields the total energy:

$$e_T = \frac{p}{\rho(\gamma - 1)} + \frac{1}{2}u^2 + Yq, \tag{2.3}$$

The reaction rate is given by:

$$\dot{W} = B\rho Y e^{-E_a/T}. \tag{2.4}$$

with pre-exponential factor B, heat of reaction q and activation energy E_a. The ideal gas law is used to find the temperature.

2.4 Time and length scale definitions

The acoustic timescale refers to the time it takes for a mechanical disturbance, like a compression or expansion wave, to travel through some characteristic length l at the local speed of sound a. It therefore describes the time required to induce fluid motion. In the plateau and gradient model developed by Kurtz and Regele [31, 32] the plateau length was used as the characteristic length scale. With this approach the local acoustic time can be defined as:

$$t_a = \frac{l}{a} = \frac{l_p}{\sqrt{\gamma R T_p}}. \tag{2.5}$$

An autoignitive reactive mixture can be described by three basic timescales: the halfreaction time, ignition delay time, and excitation time. The excitation time τ_e is roughly defined as the time it takes for a reactivemixture to fully react once the reaction has initiated after the ignition delay time τ_i has elapsed [22, 6, 17]. Since there are no distinct start and end times for chemical reactions, both can be derived from the half-reaction time τ_r at which half of the fuel has been consumed $Y_{0.5} = 0.5$.

As pictured by Figure 2.1, given the slope at the half reaction time $dY_{0.5}/dt$, the excitation time can be linearly extrapolated. The ignition delay time is then given by $\tau_i = \tau_r 0.5\tau_e$.

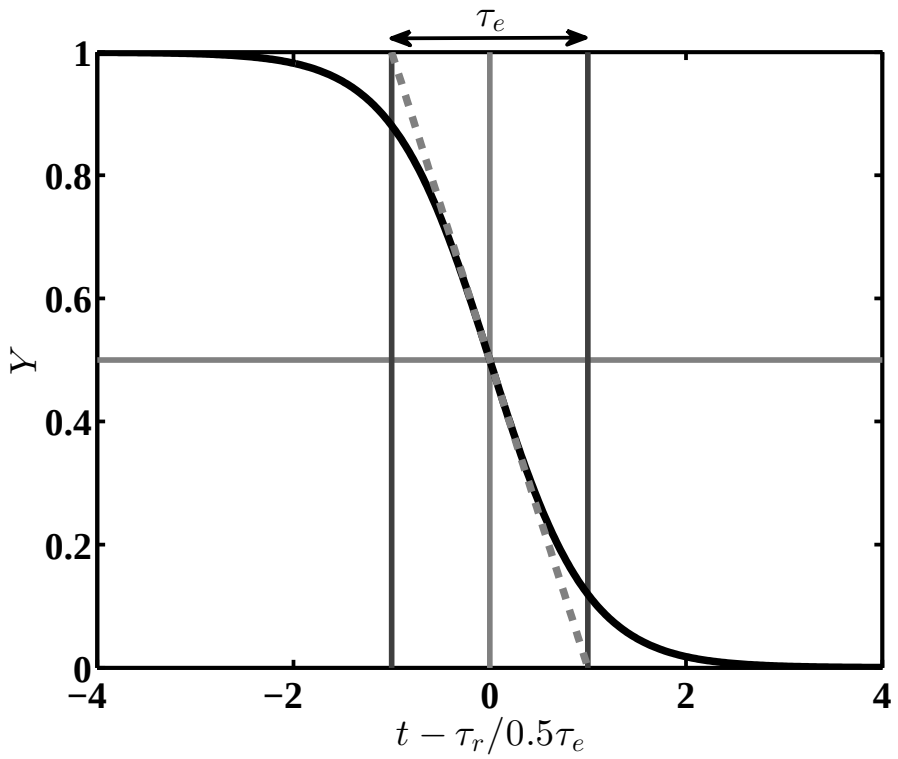

Figure 2.1 Schematic plot of fuel consumption and derivation of reaction time scales.

In previous work Kurtz and Regele [31, 32] use excitation-to-acoustic timescale ratios in order to characterise the influence of a temperature plateau at a hotspot core on the overall reaction behaviour of a hotspot. These excitation-to-acoustic timescale ratios can be defined as:

$$\frac{\tau_e}{t_a} = \frac{\tau_e a}{l_p} = \frac{L}{l_p}. \tag{2.6}$$

Here L represents the distance an acoustic wave travels during the excitation time. When the excitation-to-acoustic timescale ratio is small, $\tau_e \ll t_a$, the hotspot remains inertially confined during the reaction, resulting in a constant volume reaction. If the excitation-to acoustic timescale ratio is large, $\tau_e \gg t_a$, the hotspot is inertially unconfined and reacts at nearly constant pressure. If the timescale ratio is $\mathcal{O}(1)$, $\tau_e \approx t_a$, partial inertial confinement occurs and compression waves are created.

Viscous and conductive timescales, $\tau_v = l^2/\nu_0$ and $\tau_c = l^2/\kappa_0$, have been defined by Kassoy [24] where the characteristic dynamic viscosity and thermal diffusivity are given by ν_0 and κ_0, respectively. Both can be rewritten in terms of the acoustic Reynolds number and Prandtl number, $Re_a = l \cdot a_0/nu_0$ and $Pr = \nu_0/\kappa_0$. The viscous and conductive timescales may be written in terms of these nondimensional parameters:

$$\tau_v = \frac{l^2}{\nu_0} = Re_a \; t_a, \tag{2.7}$$

$$\tau_c = \frac{l^2}{\kappa_0} = Re_a \; Pr \; t_a. \tag{2.8}$$

2.5 Problem Statement

Linear temperature gradients and linear temperature gradients with plateaus constitute the bounding temperature profiles that represent more realistic temperature profiles. In order to account for and characterise these limiting behaviours and also analyse the behavioural dependence on smooth temperature changes between these limits, a newsuperelliptic model is proposed. The model is constructed to fulfil the following qualities.

- A zero temperature gradient should be given at the peak temperature in the hotspot centre.
- No discontinuities should exist within the hotspot temperature profile. The hotspot body can be described by a linear temperature gradient. A model for the hotspot core therefore needs to be able to transition smoothly into the outer gradient (body) for all theoretically possible connecting temperature gradients.
- It should be possible to create a wide range of hotspot core sizes so that hotspots exhibiting no, partial, or full inertial confinement may be modelled.

Simple mathematical expressions such as sine waves or quadratic polynomials cannot necessarily fulfill all these qualities. For a given interval $0 < x < l$ that is supposed to describe the hotspot

core region, the gradient covered by a quadratic function will only range from 0 to $2al$ and from 0 to $a \cdot cos(al)$ for a sine function. The gradients in the hotspot body that these core representations could smoothly connect to is therefore limited.

Another possible approach is to represent hotspots with more complex, higher order polynomials. While this would make it possible to model a temperature profile with great detail and account for all of the criteria mentioned above, the approach is underconstrained by the number of unknown polynomial coefficients that are introduced. One of the advantages of the previously used plateau and gradient model is that it utilises only two parameters, the plateau temperature and length.

A superellipse provides a new approach to combine all of these qualities, while minimising the number of parameters. In general the coordinates in a superellipse are given by:

$$\left(\frac{x}{a}\right)^n + \left(\frac{y}{b}\right)^m = 1 \tag{2.9}$$

where a and b are the foci locations in the x- and y-directions, respectively. The exponents n and m can be any finite positive number. For $n = m = 2$ Equation 2.9 represents a regular ellipse and if additionally $a = b$ a circle. Figure 2(a) shows the figures created by a superellipse for $a = b = 1$ and varying superelliptic exponents $n = m$ ranging from 1 to ∞. It can be seen that growing exponents lead to flatter, wider plateau-like regions.

Instead of using the two generic variables x and y, we can substitute the targeted variables in a onedimensional hotspot, the temperature T^e and location x, leaving four generic parameters a, b, n and m. The foci locations a and b can then be translated to an elliptic length l_{ell} and temperature ΔT_{ell} , leading to:

$$\left(\frac{x}{l_{ell}}\right)^n + \left(\frac{T^e}{\Delta T_{ell}}\right)^m = 1. \tag{2.10}$$

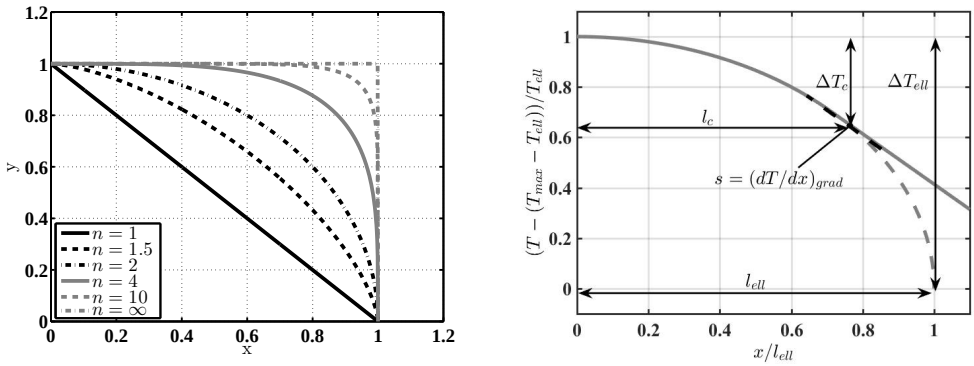

(a) (b)

Figure 2.2 (a) Evolution of superellipse for changing parameter n; (b) illustration of superelliptic hotspot parameters.

Equation 2.10 can be rearranged in order to give a temperature distribution throughout the elliptic peak. From this the temperature distribution and the temperature gradient are expressed as:

$$T^e(x) = \Delta T_{ell}\left(1 - \left(\frac{x}{l_{ell}}\right)^m\right)^{1/n}, \tag{2.11}$$

$$T^{e'}(x) = -\frac{n\Delta T_{ell}}{mx}\left(\frac{x}{l_{ell}}\right)^n\left(1 - \left(\frac{x}{l_{ell}}\right)^n\right)^{\frac{1-m}{m}}. \tag{2.12}$$

Now a temperature profile for a hotspot with rounded peak can be derived. In addition to the maximum hotspot temperature T_{max}, hotspot plateau or core length l_c and gradient $\left(\frac{\partial T}{\partial x}\right) = s$, from the plateau and gradient model, we can now prescribe a hotspot core temperature drop-off ΔT_c and superelliptic exponents n and m to describe the curvature of the temperature profile. Figure 2.2(b) shows a diagram of the hot spot model where ΔT_c is basically the temperature difference between the maximum temperature and the temperature at which the the slopes from the superellipse and constant gradient region are matched. In order to retrieve the semi-minor and semi-major axis of the super-ellipse, we set boundary conditions on Equations 2.11 and 2.12 to obtain ΔT_{ell} and l_{ell} in terms of ΔT_c and l_c. We prescribe a continuous slope $T^{e'}(x) = s$ and $T^e(x) = \Delta T_{ell}\Delta T_c$ at $x = l_c$.

For a single super-elliptic exponent $n = m = n_{ell}$, we can then derive an implicit formulation for the ratio l_c/l_{ell}, as well as an expression for ΔT_{ell}.

$$f(s, \Delta T_c, l_c, n_{ell}) \equiv \frac{\Delta T_c}{l_c} \left(\frac{l_c}{l_{ell}}\right)^{n_{ell}} \left(1 - \frac{l_c}{l_{ell}}\right)^{\frac{1-n_{ell}}{n_{ell}}} \left\{1 - \left[1 - \left(\frac{l_c}{l_{ell}}\right)^{n_{ell}}\right]^{\frac{1}{n_{ell}}}\right\}^{-1}, \tag{2.13}$$

$$\Delta T_{ell} = \Delta T_c \left\{1 - \left[1 - \left(\frac{l_c}{l_{ell}}\right)^{n_{ell}}\right]^{\frac{1}{n_{ell}}}\right\}^{-1}. \tag{2.14}$$

Under the condition that $f(s, \Delta T_c, l_c, n_{ell}) = 0$, l_{ell} and ΔT_{ell} can be found. In order for a solution to exist, $\lim_{l_{ell}\to\infty} f = 0$ needs to exist, imposing the condition:

$$s \leq -\frac{n_{ell}\Delta T_c}{l_c} \tag{2.15}$$

on the choice of possible parameters. Finally the initial temperature distribution throughout the hotspot is then given by:

$$T(x) = \begin{cases} T_{max} - \Delta T_{ell} + T^e(x) & , x < l_c \\ T_{max} - \Delta T_c + s(x - l_c) & , l_c \leq x < l_h \\ T_a & , l_h \leq x \end{cases} \tag{2.16}$$

Here T_a is the ambient temperature surrounding the hotspot, and l_h the overall hotspot length given by $l_h = (T_{max}\Delta T_c T_a)/s + l_c$. Finally the independent variables for the superelliptic model are T_{max}, l_c, s, ΔT_c and n_{ell} , in contrast to T_{max}, l_p and s for the plateau and gradient model, where the plateau length l_p corresponds to the core length l_c in the limit $n_{ell} = \infty$ and $\Delta T_c = 0$.

In this current investigation on the superelliptic model, the changing reaction behaviour for hotspots with rounded peaks is compared to the results obtained by Kurtz and Regele [31, 32] for a simpler plateau and gradient model. A plateau and gradient approximation for an example hotspot can be seen in Figure 2.3.

The model reactive mixture is given by a stoichiometric H_2-air mixture with a one-step Arrhenius reaction. Table 2.1 gives the reaction parameters obtained from Bane [4], with respect

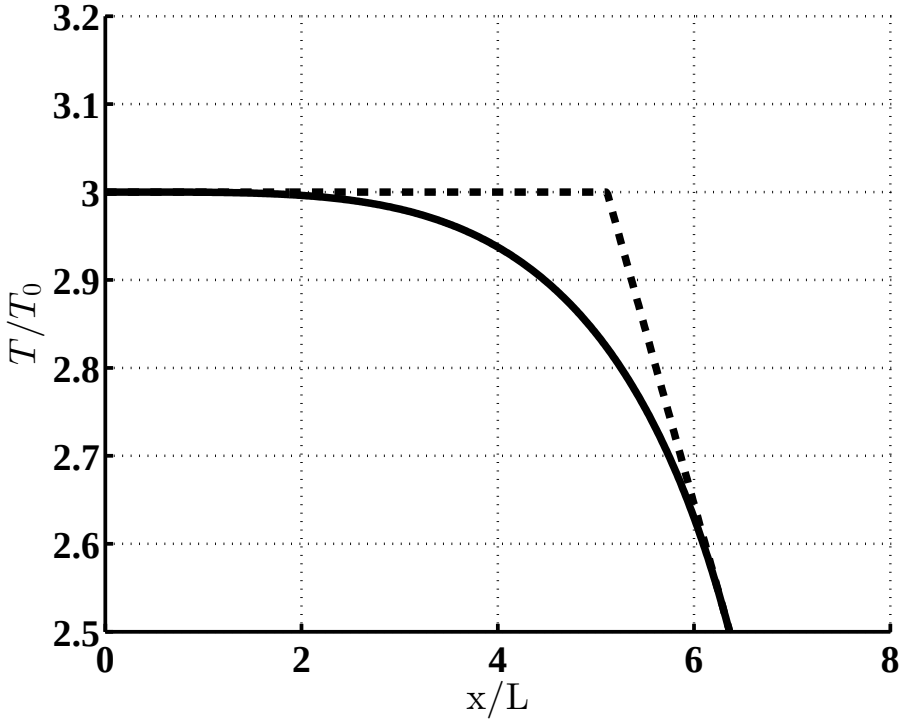

Figure 2.3 Normalised temperature distribution at hotspot core for continuous (*solid*) and plateau-gradient (*dashed*) temperature profile.

to a reference state. The universal gas constant R is calculated from the weighted average of a stoichiometric H_2air mixture.

For all cases the following applies to the respective initial conditions. The initial pressure is constant at 1 atm. At the peak the temperature and density at the hotspot centre are $T_{max} = 1260$ K and $\rho_{max} = 0.24$ kg m^{-3}, respectively. The ambient conditions are $T_a = 840$K and $\rho_a = 0.36$ kg m^3. A gradient of $s = 168$ K mm^1 is chosen, which is too steep to create strong compression or shock waves on its own, but is a gradient suggested in [5] to be a realistic gradient observable in IC engines.

Superelliptic exponents ranging from 1 to 100 are investigated, where $n_{ell} = 1$ represents the gradient only bounding temperature profile and $n_{ell} = 100$ the plateau and gradient bounding

Table 2.1 Values of pre-exponential factor, activation energy, and heat of reaction presented in terms of the given reference state.

Parameter	Value
P_0	1 atm
T_0	300 K
γ	1.4
R	398 J/(kg K)
a_0	347 m/s
B	$2.26e+9$ (s^{-1})
E_a	$33\gamma RT_0$
q	$12\gamma RT_0$

temperature profile. As illustrated in Figure 2.2(a), the elliptic exponent is varied to explore the behaviour of smooth temperature profiles that lie in between these two bounds. For each exponent, an excitation-to-acoustic timescale ratio is calculated. Table 2.2 gives a list of all exponents n_{ell} and corresponding timescale ratios for all cases. ΔT_c and l_c are adjusted in such a way that for all n_{ell} the dependent variables ΔT_{ell} and l_{ell} are kept constant and that for large n_{ell} the resulting plateau has a length of $10L$. In this case the reference plateau and gradient case obtained from the superelliptic model then correlates to the fully inertially confined case investigated in previous studies [31, 32]. In order to fulfill Equation 2.15 for all n_{ell} , the constant reference dependent variables are chosen $\Delta T_{ell} = 571.2$ K and $lell = 3.4$ mm. This ensures that the underlying superellipse describing the core temperature variation varies only in terms of its exponent n_{ell}.

Note that the T_{max}, ΔT_c and l_c can be additional parameters to explore to fully describe the ignition behaviour of smoothly varying temperature profiles. Variation of T_{max} is not anticipated to alter the behaviour observed in this work because the results are normalised by acoustic and excitation timescales, which are set by the maximum temperature. As for n_{ell}, the variation of n_{ell} still shows the influence of smooth temperature variation on its own. In this work, we have chosen constant values of ΔT_{ell} and l_{ell} to capture these effects while satisfying the constraint Equation 2.15. A full exposition of the effects of varying these other parameters independently awaits further investigation.

Table 2.2 Investigated superelliptic parameters and corresponding plateau-gradient model acoustic timescale ratios.

n_{ell}	τ_e/t_a	n_{ell}	τ_e/t_a
1	∞	1.225	0.74
1.015	9.7	1.25	0.67
1.02	7.3	1.275	0.62
1.04	3.7	1.5	0.38
1.06	2.5	4	0.15
1.15	1.06	10	0.12
		100	0.10

The use of the reactive Euler equations and thus omission of transport terms is validated by a comparison of the timescales of interest. At the reference state the acoustic Reynolds and Prandtl numbers are nearly $22,000$ and 0.7, respectively. Substituted in Equations 2.7 and 2.8 the resulting viscous and conductive timescales are four orders of magnitude larger than the acoustic time, leaving all other timescales of interest within one order of the acoustic time. This validates the use of the reactive Euler equations to model the timescales of interest.

2.6 Numerical Method

The parallel adaptive wavelet collocation method (PAWCM) [27, 65] is used to solve the governing equations. A revised hyperbolic solver developed specifically for the PAWCM is used to stabilise shocks and contact discontinuities [48]. Symmetric boundary conditions are used on the left boundary and outflow conditions on the right boundary. The spatial discretisation is second order accurate in smooth regions and reduces to between first and second order in regions with shock or contact discontinuities. A van Leer flux limiter minimises numerical diffusion and maintains nonlinear stability [64, 1].

Abase grid of 20 grid points is used with 13 levels of refinement, resulting in a maximum of $81,920$ effective grid points. The grid spacing corresponding to the highest refinement level is $\Delta x \approx 1.8E-04$ mm. This resolution is necessary in order to fully resolve the peak pressure at the von Neumann spike with an error of less than 1% [31].

2.7 Results

In order to verify the results presented in this work are accurate, the $n_{ell} = 4$ case was run until a steady detonation wave was formed. The CJ detonation Mach number can be found using [61]:

$$M_{CJ} = \left(\sqrt{\frac{q\,(\gamma^2 - 1)}{2a_1^2}} + \sqrt{1 + \frac{q\,(\gamma^2 - 1)}{2a_1^2}} \right) \tag{2.17}$$

where q is the heat of reaction and a_1 is the speed of sound in the reactants. The propagation Mach number M_{CJ} measured numerically is found to be within 0.31% of the theoretical value of 3.19. The corresponding peak pressure for a detonation wave propagating in the surrounding constant temperature region is 11.6 atm. The CJ Mach number and post-shock pressure are lower than the typical value of 5 because the reactive mixture is at an elevated temperature.

Figure 2.4 shows xt diagrams for the simulation results obtained for superelliptic hotspots with exponents $n_{ell} = 1.015$, 1.15 and 4. These cases correspond to acoustic timescale ratios $\tau_e/t_a = 9.7$, 1.06 and 0.15 exhibiting little, partial and full inertial confinement, which are timescale ratios similar to those presented in Kurtz and Regele [31, 32]. For each case the xt diagrams show the contours of the temperature and pressure throughout the domain. The time is normalised by the isochoric half-reaction time at the maximum initial temperature in the hotspot and the distance is normalised by the length L. *Solid*, *dashed* and *dot-dashed* white lines represent the demarcation between the reacted and unreacted material in the unconfined, partially confined and fully confined cases, respectively. In order to improve the visualisation of the pressure variation in the detonating case away from the detonation itself, the pressure in Figure 2.4(f) has been capped at 7 atm.

2.7.1 Dependence on superellipse exponent

In Figure 2.4(a) it can be seen that the reaction in the unconfined case starts slightly after the isochoric half reaction time, when there is a sudden increase in temperature due to the chemical heat release at $t/\tau_r \approx 1.2$, closer to the isobaric half reaction time. The reaction front then propagates down the temperature gradient. As the initial gas temperature gets lower, the reaction front slows down as indicated by the increase in slope. The maximum pressure created in this case is 2.2atm,

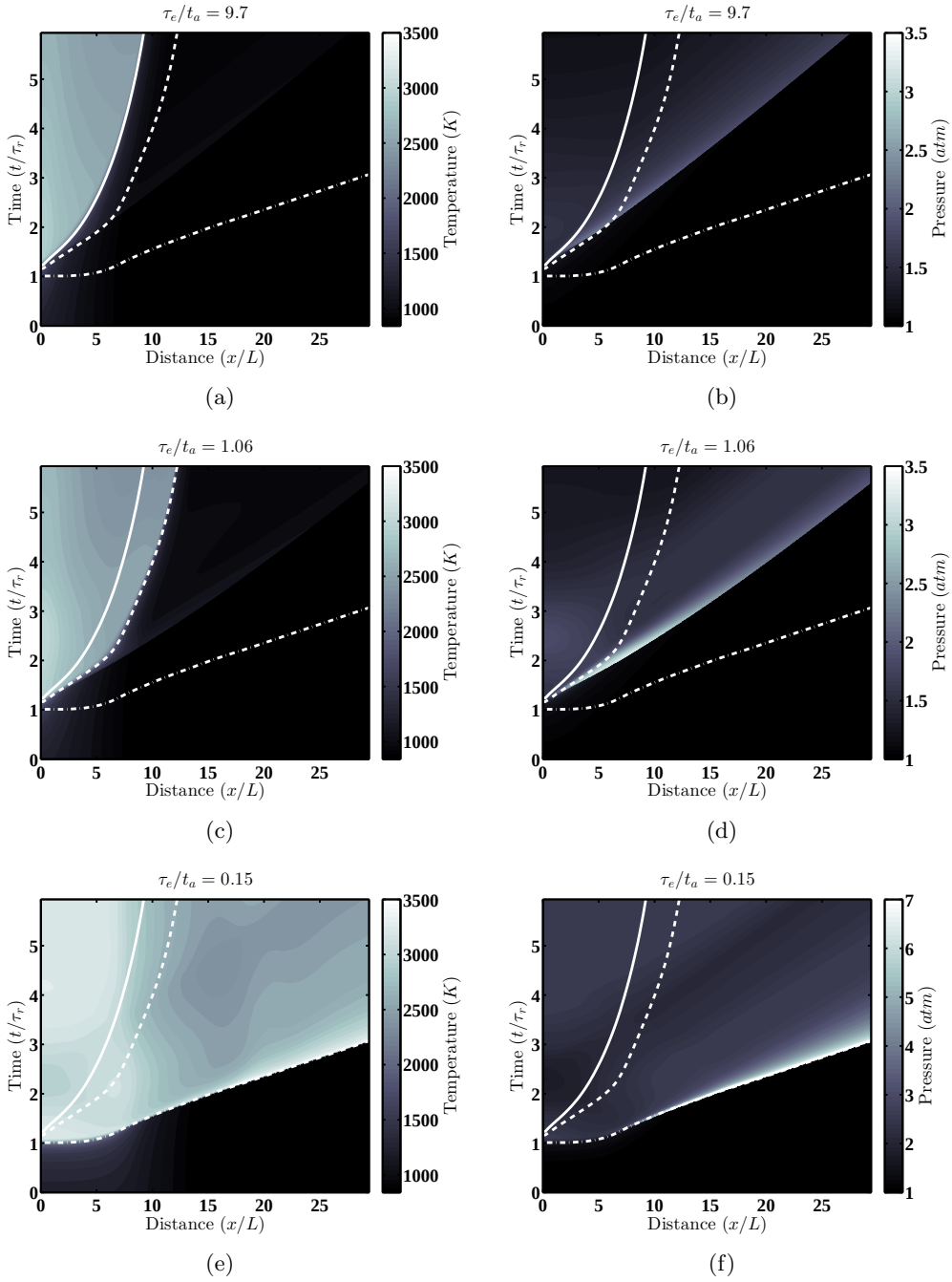

Figure 2.4 Contour plot of temperature (a, c, e) and pressure (b, d, f) over time throughout the domain. Lines indicated the interface between reacted and unreacted material for each reference timescale ratio 9.7 (*solid*), 1.06 (*dashed*) and 0.15 (*dot-dashed*).

which occurs at $t/\tau_r = 1.9$. In Figure 2.4(b) it can be seen that an incidental shock is sent out as the mixture ignites around $1.2\tau_r$. Initially the peak pressure in this shock is 1.47atm. It stays decoupled from the reaction front (solid white line) at all times.

Figure 2.4(c) shows the temperature contour for the partially confined case. Heat release from the reaction begins at $t/\tau_r \approx 1.1$, slightly after the isochoric half reaction time has passed. Compared to the unconfined case it can be seen that the half reaction front progresses initially faster. The corresponding pressure plot, Figure 2.4(d), shows that initially the reaction front couples to the incidental shock. Compared to Figure 2.4(b) the incidental shock is stronger and reaches a peak pressure of 1.85 atm at $t/\tau_r \approx 1.2$, a 25% increase as compared to the unconfined case. As time progresses this difference becomes even more apparent. In the coupled shock and reaction front the peak pressure builds up to 2.82 atm by $t/\tau_r \approx 1.5$, whereas in the unconfined case it only reaches a pressure of 1.98 atm, a 50% difference. The stronger incidental shock thus preheats the material in the gradient region more, reducing the ignition delay time and triggering the reaction, which leads to the initial coupling of shock and reaction front. As the shock proceeds further down the temperature gradient of the hotspot body, it is no longer strong enough to preheat the material enough to lead to an immediate reaction. At about $t.\tau_r \approx 2$ the reaction front and shock therefore decouple again. Figure 2.4(e) and 2.4(f) show the temperature and pressure for the confined case with $\tau_e/t_a = 0.15$. In this case the shock stays coupled at all times, resulting in a detonation. Compared to the partially and unconfined cases, the reaction starts right after the isochoric ignition delay time and the heat release therefore is observable right at $t/\tau_r \approx 1$. At $t/\tau_r \approx 1.2$ and 1.5 the peak pressures reach 3.34 atm and 5.54 atm. This significantly higher pressure rise is able to trigger an immediate reaction even as the shock proceeds into the colder domain. The reaction front and shock remain coupled and lead to a detonation.

Figure 2.5 show the results for a range of superelliptic exponents and thus excitation-to-acoustic timescale ratios. The cases are grouped according to the degree of inertial confinement. For each of the unconfined, partially confined and confined cases, the initial temperature profile, trajectory of the half reaction front and the gas velocity of at half reaction front are given. Similar to the

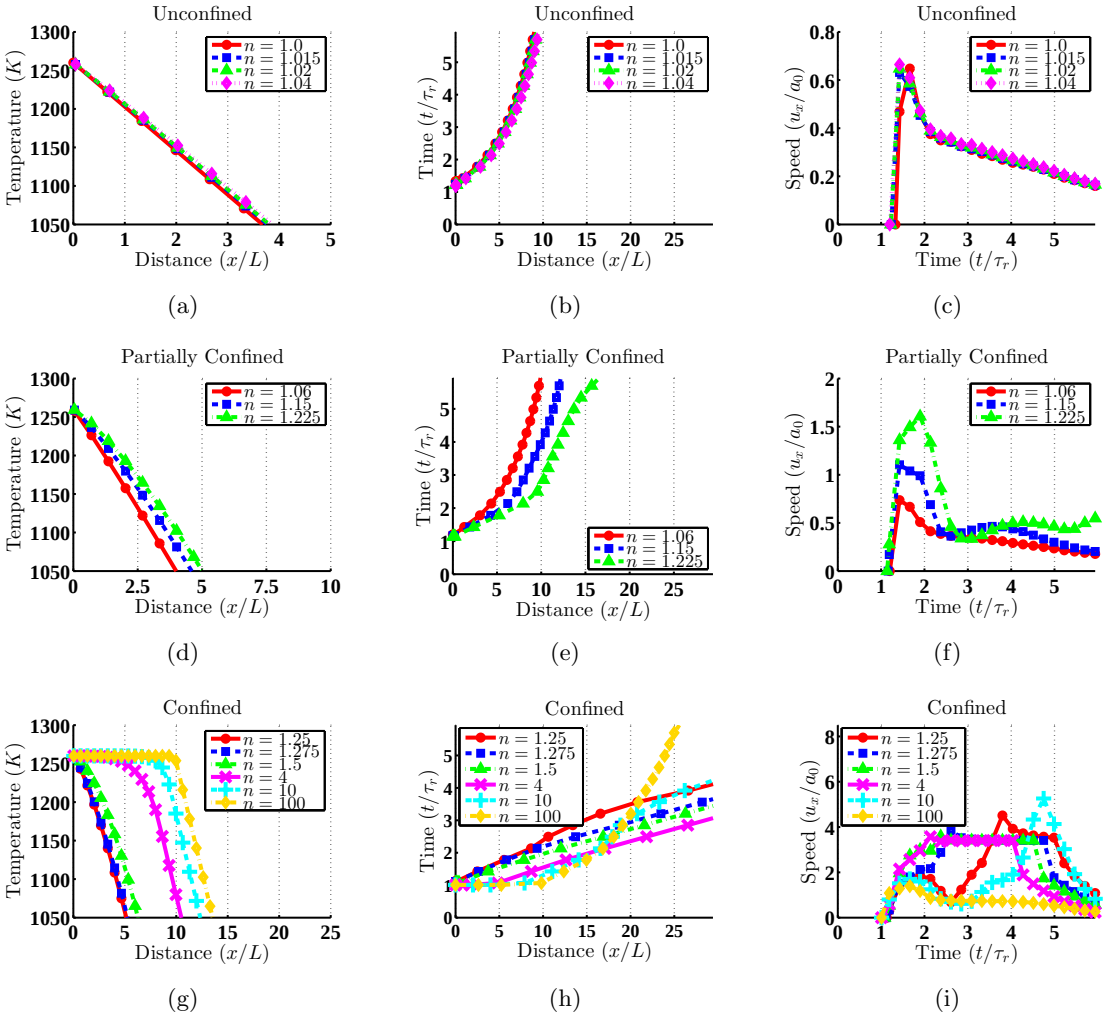

Figure 2.5 Initial temperature distribution zoomed in on the hotspot core to highlight smooth temperature variation at the centre (a, d, g), trajectory of half-reaction front (b, e, h) and gas velocity at half-reaction front (c, f, i) for unconfined (ac), partially confined (df) and confined (gi) cases, given by the varying superelliptic exponents.

contour plots given in Figure 2.4, time and length are normalised by the isochoric half reaction time and length L. The velocity at the propagation front is normalised by the reference speed of sound a_0. The initial temperature profiles are shown at the hotspot centre only in order to show the minute differences between cases and especially for cases with nell close to unity. Partially confined cases are distinguished from unconfined cases by whether the shock and reaction fronts couple initially or not. Confined cases are distinguished from partially confined cases by whether the half reaction recouples with the shock and forms a detonation or not for exponents close to unity. Large exponents automatically resulting in excitation-to-acoustic timescale ratios on the order of 0.1 are considered confined, independent of whether a detonation is formed or not, since these timescale ratios will result in a constant volume reaction throughout the hotspot core.

For the unconfined cases shown in Figure 2.5(a),2.5(b),2.5(c), it can be seen in Figure 2.5(a) that the initial temperature profile varies only slightly between each case with variations on the order of 0.1%. The excitation-to-acoustic timescale ratio of the plateau however varies by almost one order of magnitude from 9.7 to 3.7, excluding the gradient only case, which has a theoretical timescale ratio of ∞, due to the lack of a finite plateau size. Similarly the half reaction front trajectories and propagation speed curves coincide, showing the same reaction behaviour for all cases. As observed in Figure 2.4(a) and 2.4(b), without the half reaction front coupling to the shock, it immediately begins to decelerate. This becomes even more apparent when looking at the plot of the propagation speed at the half reaction front, Figure 2.5(c). The velocity initially peaks at $t/\tau_r \approx 2$, when the fast incidental shock emitted at the hotspot centre passes through the half reaction front. After this peak the propagation velocity starts to decrease linearly, as the reaction front proceeds down the linear initial temperature gradient into the colder gas.

In the partially confined cases, illustrated in Figure 2.5(d), the timescale ratios vary from 2.5 to 0.74 and a slightly different behaviour is observed. Initially the shock and half reaction front couple and they stay coupled longer for an increasing level of confinement (smaller τ_e/t_a or larger n_{ell}). For $n_{ell} = 1.06$, corresponding to $\tau_e/t_a = 2.5$ they decouple after $1.5\tau_r$ (*circle*), which can also be seen in Figure 2.4(c) and 2.4(d). For $n = 1.225$ ($\tau_e/t_a = 0.74$) they remain coupled until $2\tau_r$

(*diamond*). In the cases with exponents 1.06 and 1.15 the half reaction follows a similar trajectory to the unconfined cases once shock and reaction decouple. In the $n_{ell} = 1.225$ case the reaction front starts to accelerate again at $5\tau_r$ as shown in the trajectory and propagation speed plots, Figure 2.5(e) and 2.5(f). In contrast to the unconfined cases, the partially confined cases show a second acceleration in the reaction front for cases $n_{ell} = 1.15$ and $n_{ell} = 1.225$. In the latter case a tertiary acceleration can be observed in Figure 2.5(e) at $t5\tau_r$. In general, increasing exponents increase the confinement of the core region, which then increases the strength of the initial shock. Stronger shocks preheat the reactive mixture more and thereby increase the peak velocity. In the unconfined cases the peak speed is almost constant for all exponents at around $u_x/a_0 = 0.65$, which suggests that the compression or shock wave created from the core region reaction has little if any effect on the surrounding gradient region. On the other hand, Figure 2.5(c) shows that the peak velocity for the partially confined cases range from 0.75 to 1.7, demonstrating a clear dependence on the core profiles when the excitation-to-acoustic timescale ratios are $\mathcal{O}(1)$.

Fully confined cases, shown in Figure 52.5(g),2.5(h),2.5(i), have plateau excitation-to-acoustic timescale ratios ranging from 0.67 to 0.1. The initial temperature profiles in Figure 2.5(g) show that as the exponent increases the size of the plateau increases until a plateau-like hotspot centre is created and surrounded by a gradient region. As n_{ell} approaches ∞, the hotspot approaches the plateau and gradient model, which can be seen in the cases of $n_{ell} = 10$ and 100 (*plus*, *diamond*). Figure 2.5(h) shows the trajectories of the half reaction fronts. It can be seen that in all cases except for the plateau and gradient case, $n_{ell} = 100$, the reaction front and shock couple to form a detonation. Just a slight increase in the exponent from 1.225 ($\tau_e/t_a = 0.74$) in the partially confined case to 1.25 ($\tau_e/t_a = 0.67$) in the confined case leads to detonation formation from a secondary explosion. In the cases with exponents 1.275, 1.5 and 4 (*square*, *triangle*, *x*) detonation formation occurs immediately after ignition, which can be inferred from the linear trajectory of the half reaction front (Figure 2.5(h)) and the velocity at the reaction front (Figure 2.5(i)). In these cases no initial peak from the incidental shock passing through the reaction front is present. Instead, the shock is further accelerated by the reaction and transitions into a steady detonation with constant

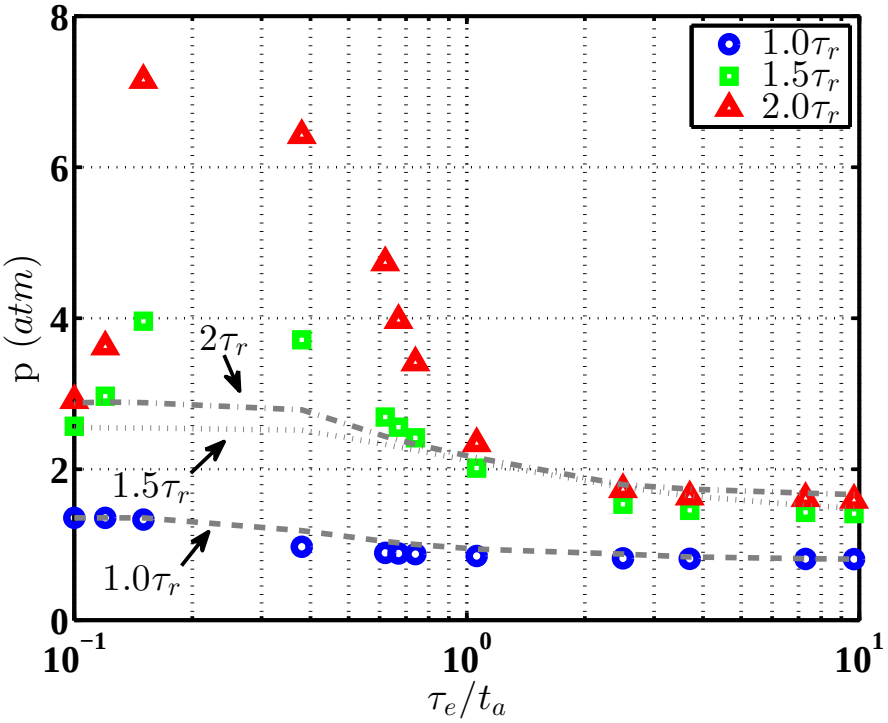

Figure 2.6 Peak pressure in incidental compression wave emitted by hotspot core at times $1.0\tau_r$, $1.5\tau_r$ and $2.0\tau_r$ for superelliptic hotspots of varying reference timescale ratios (*circle*, *square*, *triangle*) and respective plateau and gradient model hotspots (*dash*, *dot*, *dot-dash*).

propagation velocity. The latter drop off in velocity is due to the reaction front leaving the domain. Cases with exponents of 1.25 and 10 do not immediately transition to detonations. This can easiest be seen in the velocity Figure 2.5(i). In these cases there is an initial peak in velocity from the original ignition and then the reaction decouples from the shock. Later the reaction catches up to the shock and forms a detonation at $3.8\tau_r$ and $4.7\tau_r$ for $n_{ell} = 1.25$ and 10, respectively. For the plateau and gradient case given by the exponent of $n_{ell} = 100$ (*diamond*) the reaction does not transition to detonation. While the shock and reaction are coupled initially, the shock wave does not adequately preheat the mixture to a temperature such that a localised explosion will occur and form a detonation wave.

For each case, Figure 2.6 shows the maximum pressure inside the domain at 1, 1.5 and 2 times the half reaction time τ_r. The results are presented in terms of the corresponding plateau excitation-to-acoustic timescale ratios listed in Table 2.2. Not shown in Figure 2.6 are the pressures for the gradient only case, since the theoretical ratio τ_e/t_a would be ∞ and the pressures produced by this case are similar to some of the larger timescale ratio cases. The time τ_r shows the initial stages of compression wave formation. Later times, $1.5\tau_r$ and $2\tau_r$, correspond to the compression waves travel inside the hot spot core and linear temperature gradient regions. For the partially and unconfined cases, $\tau_e/t_a > 0.74$, the initial pressure rise forms a gradually increasing compression wave, rather than a shock. In all other cases the peak pressures correspond to post-shock pressures.

For the unconfined cases with timescale ratios greater than unity, the peak pressure is nearly identical at each of the different times, which is consistent with the similar reaction behaviours observed in Figure 2.5(a),2.5(b),2.5(c). When partial inertial confinement is exhibited by the hotspot core, the maximum pressure grows. For the case with an excitation-to-acoustic timescale ratio of 1.06 the peak pressures at times $1.5\tau_r$ and $2\tau_r$ reach values of 2.9 and 3.3 atm. This trend of increased pressure in the shockwaves emitted from the hotspot core continues for increasing inertial confinement and decreasing excitation-to-acoustic time ratios. The maximum pressure at r becomes nearly independent of excitation-to-acoustic timescale ratios for $\tau_e/_t a < 0.15$. This occurs because the temperature profiles for these timescale ratios correspond to exponents $n_{ell} > 4$ where the reaction is dominated by a constant volume reaction inside of a large temperature plateau. At later times the peak pressure varies significantly between the different inertially confined cases. The plateau and gradient model alone predict a smaller increase in pressure, and thus less compressive heating. Smaller hotspots, given by smaller exponents, lead to a smaller increase in pressure. This suggests that the growth in strength of the shock happens inside the hot spot core where the temperature gradient changes gradually.

The grey dashed, dotted and dot-dash line in Figure 2.6 mark the maximum pressures in the domain for the plateau and gradient reference cases at times τ_r, $1.5\tau_r$ and $2\tau_r$ respectively. It can be seen that in comparison to the superelliptic model the plateau and gradient model predicts a

similar initial pressure rise at τ_r for all cases. At $t = \tau_r$ only the hottest material at the hotspot peak has reacted and the pressure rises mainly inside the hotspot core. This initial pressure rise sends pressure waves into the regions of changing gradient in the superelliptic model cases and directly into the gradient region in the plateau and gradient model cases. At $t = 1.5\tau_r$ more differences become apparent. For the unconfined cases, timescale ratios larger than 2, the plateau and gradient model captures the peak pressure fairly accurately with only a slight over-prediction.

As the timescale ratios decrease and the inertial confinement increases, a larger rise in pressure can be seen in the superelliptic case. As the initial compression waves travel through the region of changing temperature gradient, rather than constant gradient, more pressure builds up. Until a point, the difference between the pressure rise in the superelliptic and the plateau and gradient only case grows larger as the reference timescale becomes smaller. The difference is the greatest in the cases with timescale ratios equal to 0.38 and 0.62. For timescale ratios smaller than the 0.38 case the peak pressure approaches the plateau and gradient model again. This effect becomes even more significant at $2\tau_r$. For timescale ratios larger than unity it can be seen that for the unconfined and partially confined cases, the plateau and gradient, as well as the more realistic superelliptic model lead to similar pressure rises. For partially and fully confined cases with timescale ratios smaller than unity, the difference between the pressure rise resulting from both models becomes significant. The change in gradient inside the hotspot core in partially and fully confined hotspots plays an important role in accelerating spontaneous reaction fronts to form detonation waves. This suggests that, in addition to the hotspot core size, how the temperature changes inside of the core regions can have a significant influence on the ignition behaviour.

Additional cases have been performed where the maximum temperature T_{max} is varied from $T_{max} = 840$ K to infinity where the reaction behaviour is independent of the initial temperature. It is found for realistic temperatures that the gasdynamic response of the gas is independent of the maximum temperature as long as the excitation-to-acoustic timescale ratio for the core region is the same. This suggests that the excitation-to-acoustic timescale ratio provides a universal mechanism that eliminates the maximum temperature T_{max} from the ignition behaviour.

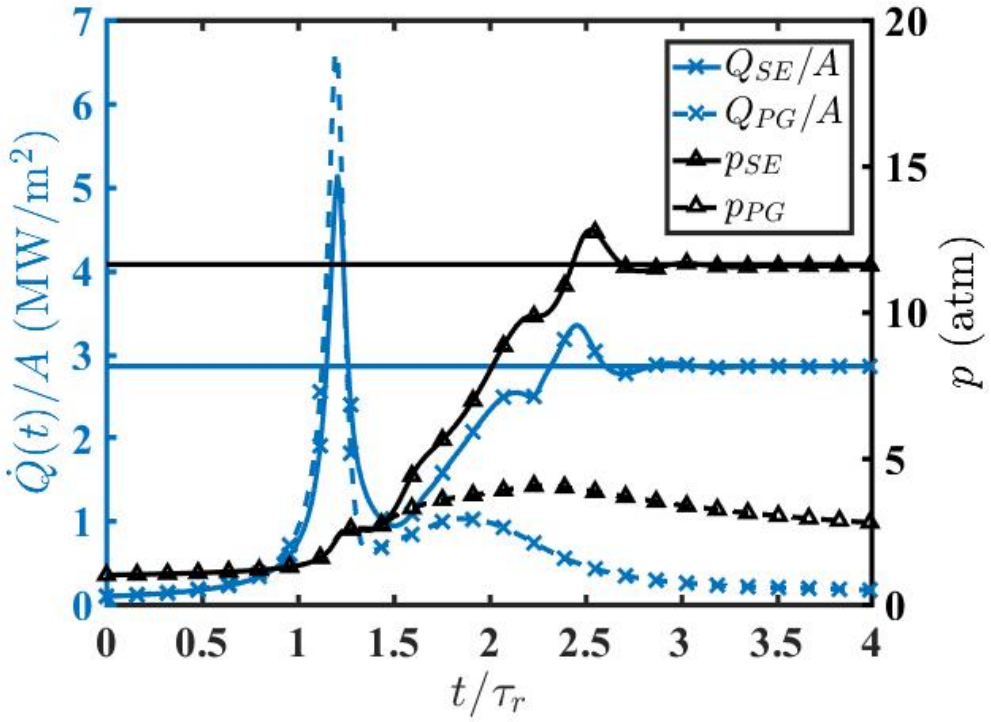

Figure 2.7 Global heat release rate per unit area (*crosses*, left y-axis) and maximum pressure (*triangle*, right y-axis) in domain for superelliptic (SE, *solid*) and plateau and gradient (PG) cases (*dash*) for ($n_{ell} = 4$) over time.

2.7.2 Effects of smooth temperature variation

In order to illustrate the difference in behaviour between the plateau-gradient (PG) and superelliptic (SE) models, the $n_{ell} = 4$ ($\tau_e/t_a = 0.15$) case, which corresponds to the highest peak pressure in Figure 2.6, can be compared with the plateau gradient case with the same timescale ratio. Figure 2.7 compares the 1-D globally integrated heat release rate ($\dot{Q}/A$) and maximum pressure between these two cases. Solid lines represent the superelliptic case, while dashed lines represent the corresponding plateau and gradient case. The two horizontal lines show the heat release per unit area of 2.85 MW/m2 and peak pressure of 11.63 atm that correspond to a steady CJ state respectively. In both cases the reaction within the hotspot core begins around $t/\tau_r = 0.93$, with the onset of an

increased global heat release rate and rising pressure throughout the hotspot core. At $t/\tau_r = 1.19$ the global heat release reaches a maximum, just after the isochoric half reaction time. Although the heat release begins very similarly for each of the two cases, the plateau-gradient model has a higher peak heat release rate than the superelliptic case. After the peak in heat release the PG model drops off more quickly than the SE model until around $t/\tau_r \approx 1.4$. For $t/\tau_r > 1.4$ the heat release rate for the SE model rises significantly faster than the PG model and eventually matches the CJ heat release rate, indicating that a detonation wave has formed. Similarly, the peak pressure for each model is nearly identical until $t/\tau_r \approx 1.4$, after which the peak pressure for the SE model continues to rise until a detonation is formed.

Since the peak pressure is nearly identical up until $t = 1.4$ and then after that the two cases reacts very differently, it is the difference in temperature profiles that causes the different behaviours. It is clear that the smooth variation in temperature inside the hot spot core facilitates the formation of a detonation wave more easily than a relatively large volume of gas reacting uniformly to produce a shock wave that compresses surrounding reactive media in a linear temperature gradient. This can be inferred by observing that the heat release for the SE model has a lower maximum with a higher minimum after the initial hot spot core reaction than the PG model. This suggests that better coupling between the reaction and pressure waves generated from the reaction occur in the SE model over the PG model.

Figure 2.8 shows the trajectories of the half reaction front and maximum pressure location with respect to the original dimensions of the hotspot. Half reaction front trajectories are indicated by x-markers and peak pressure locations are indicated by triangle markers. The trajectories of the superelliptic case are given by solid lines and the trajectories in the plateau and gradient case by dashed lines. The two vertical lines indicate the original borders of the hotspot core, gradient and ambient regions. In both cases at $t/\tau_r \approx 1.15$ a half-reaction front forms. At this time in the SE case the half-reaction front is located at $x/L \approx 2.5$, meaning that about a third of the hotspot core has reacted. In the PG case it is located at $x/L \approx 4.3$, which corresponds to roughly two thirds of the hotspot core. The remaining hot material inside the hotspot core is rapidly consumed in the

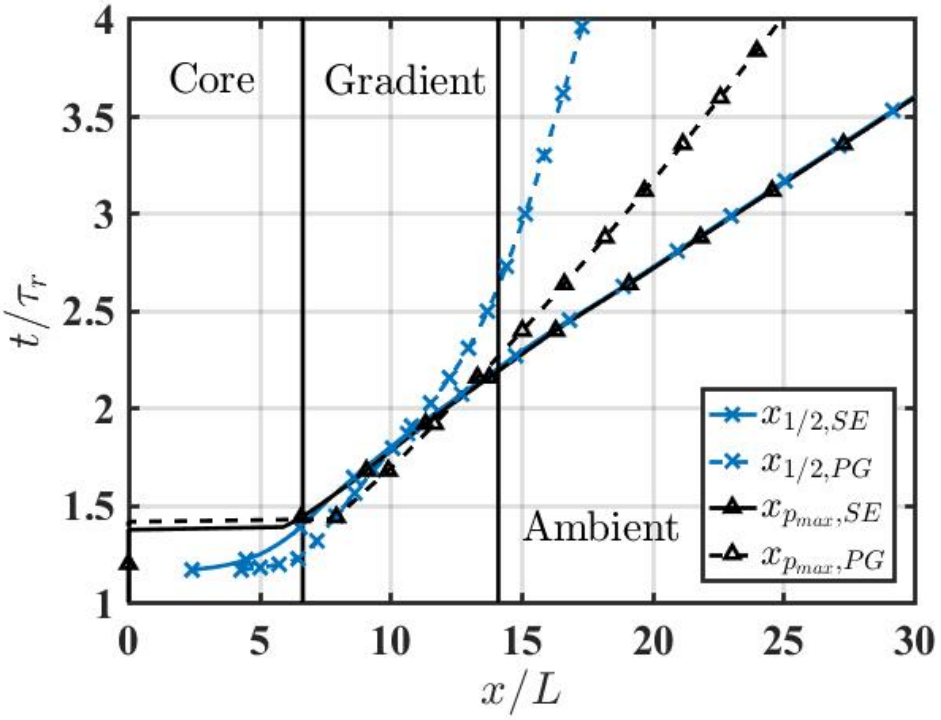

Figure 2.8 xt diagram showing the trajectories of half-reaction front (x) and location of maximum pressure (*triangle*) in respect to the original hotspot temperature profile for ($n_{ell} = 4$), for plateau and gradient (*dash*), and superelliptic (*solid*) case.

PG case by $t/\tau_r \approx 1.24$, while in the SE case it takes until $t/\tau_r \approx 1.4$. After the rapid consumption of the hotspot core in the PG the half-reaction front decelerates abruptly as it moves into the cooler gradient region, due to the sudden change in temperature gradient at this point.

Also seen in Figure 2.8, the global maximum pressure is initially located at the hotspot centre. As indicated by the nearly horizontal lines for $x_{p_{max}}$ at $t/\tau_r \approx 1.4$, the reaction grows to sufficient magnitude and the global maximum pressure moves rapidly to the outside of the core region. After this point the global maximum trajectory tracks a compression wave moving into the unreacted material. In the SE case, after the rapid movement in maximum pressure, the wave first appears inside the hotspot core region at $x/L \approx 5.9$, while in the PG case it is already in the gradient region

at $x/L \approx 7.9$. Right as the maximum pressure in the PG case shifts from the hotspot centre to the pressure wave it passes the half reaction front. The pressure wave moves with a faster velocity down through the gradient region ahead of the reaction without coupling. In the SE case the half reaction front gradually decelerates as it leaves the hotspot core. The pressure wave catches up to it around $t/\tau_r 1.54$ and reaction front and pressure wave couple just outside of the core region. This suggests that the dynamics leading to the coupling of the pressure and reaction waves mostly occurs inside the smooth temperature variation inside the hot spot core. This can be contrasted with the PG model where the two waves do not cross each other until $t/\tau_r \approx 1.45$, which is approximately 20% ($x/L = 8$) into the gradient region. This suggests that the reactive media will be significantly cooler, which may prohibit the coupling from occurring. This is supported by the fact that the pressure up until this time (Figure 2.7) is exactly the same in both cases.

As performed in Regele et al. [51] the local acoustic to heating timescale ratio of a moving wave can be evaluated to further investigate the different ignition dynamics. Since the excitation time can be assumed to be much smaller than the induction time $\tau_e \ll \tau_i$, the heat release throughout a small fluid volume of length Δx at x_0 can be assumed to occur between $\tau_i(x_0)$ and $\tau_i(x_0 + \Delta x)$. Thus the heating time in this region for a fluid volume Δx can be written as:

$$t_h = \tau_i(x_0 + \Delta x) - \tau_i(x_0). \tag{2.18}$$

The ignition delay time $\tau_i(x_0 + \Delta x)$ can be expanded using a Taylor series as:

$$t_h = \frac{d\tau_i(x_0)}{dx} + \mathcal{O}(\Delta x^2). \tag{2.19}$$

For the same fluid volume the acoustic time scale is given by $t_a = \Delta x/a(x_0)$, with the speed of sound $a(x_0)$ at x_0. The heating to acoustic time scale ratio is then given by:

$$\frac{t_h}{t_a} = \frac{d\tau_i}{dx}\frac{\Delta x}{\Delta x/a(x_0)} = \frac{a(x_0)}{u_x(x_0)}. \tag{2.20}$$

Here u_s is defined as the spontaneous wave speed $u_s = (d\tau_i/dx)^1$ as described by Zeldovich [73] and $a(x_0)$ the local speed of sound. The local heating to acoustic timescale ratio is formed at $x_{1/2}$,

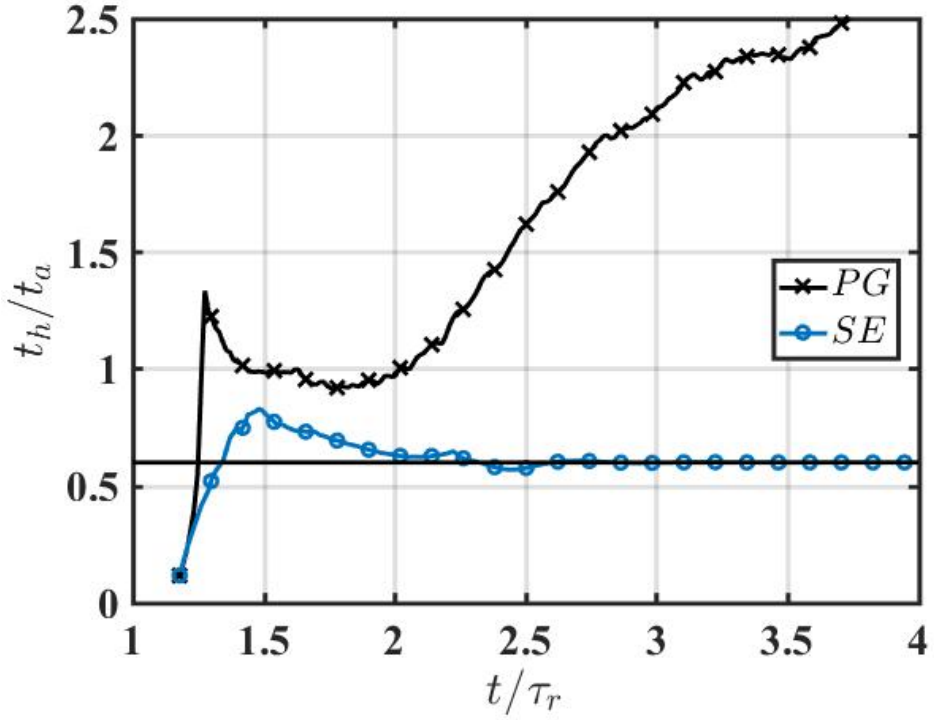

Figure 2.9 Local heating to acoustic timescale ratio evolution over time for plateau and gradient (PG), and superelliptic (SE) reaction case for ($n_{ell} = 4$).

the half reaction front location, which gives $a(x_0) = \sqrt{\gamma RT(x_{1/2})}$ and $u_s = dx_{1/2}/dt$. For a steady CJ detonation the spontaneous wave speed becomes the propagation speed of the detonation wave $D_{CJ} = a_1 M_{CJ}$. The temperature at the half-reaction location for a CJ detonation can be found in Strehlow [61]:

$$\frac{T(Y)}{T_1} = \frac{M^2\left(1+\gamma M^2+\gamma\sqrt{\left(M^2-1\right)^2-2\left(\gamma+1\right)\left(\gamma-1\right)M^2\frac{q}{a_1^2}\left(1-Y\right)}\right)}{1+\gamma M^2-\sqrt{\left(M^2-1\right)^2-2\left(\gamma+1\right)\left(\gamma-1\right)M^2\frac{q}{a_1^2}\left(1-Y\right)}} \tag{2.21}$$

Figure 2.9 shows the development of the local heating to acoustic timescale ratio over time for the SE case, marked by circles, and PG case, marked by crosses. The solid horizontal line indicates the steady CJ heating to acoustic timescale ratio at ambient conditions, given by:

$$\left(\frac{t_h}{t_a}\right)_{CJ} = \frac{a_1 M_{CJ}}{\sqrt{\gamma RT\,(y=0.5)}}. \tag{2.22}$$

Up until $t/\tau_r \approx 1.24$ the local timescale ratio grows linearly at the same rate in both the SE and PG case up to 0.32, indicating strong inertial confinement of the reaction zone. At this point in the PG case the local timescale ratio jumps to a value greater than unity $th_/t_a \approx 1.35$ at $t/\tau_r \approx 1.28$, resulting in reduced partial inertial confinement. In contrast, in the SE case a steady growth can be observed until $t/\tau_r = 1.48$ when the local acoustic to heating timescale ratio peaks at a value smaller than unity, 0.83. After the initial peak the local timescale ratio decreases in both cases. In the PG case it drops off and plateaus around 1 from $t/\tau_r = 1.44$ to 1.63, then decreases further to a minimum of about 0.9 and grows continuously after $t/\tau_r = 2$. In the SE case the local timescale ratio continuously drops after its initial peak and converges towards the steady CJ value. At $t/\tau_r = 2$, the local heating to acoustic timescale ratio of the forming detonation wave is within 5% of that of a CJ detonation. While the reaction in the PG case loses its full inertial confinement shortly after its initiation and with timescale ratios on the order of and larger than unity, the reaction in the SE case remains fully inertially confined at all times with no discontinuous changes over time.

Figure 2.9 shows that the timescale ratios are very similar while the reaction is inside the hot spot core until $t/\tau_r = 1.35$. In the PG model, for $t/\tau_r > 1.35$, the reaction becomes only partially confined, which further suggests that the temperatures are too low to support pressure-reaction coupling outside of the core region. In contrast, the SE model maintains a sub-unity timescale ratio for the duration of the ignition and thereby supports the formation of a detonation wave. After the local maximum in heat release, both cases show a reduction in timescale ratio, which indicates that the pressure wave has preheated the reactive media and increased the reaction rate. However, in the PG case, the increase in reaction rate is not substantial enough to form a detonation. This

is evidenced by the increase in the timescale ratio for $t/\tau_r > 1.8$; whereas, in the SE model, the timescale ratio reduces to the detonation limit.

2.8 Conclusions

A new superelliptic model has been proposed and investigated. It is shown that the model provides a way to model not only linear temperature gradients and gradients with a constant temperature plateau, but all of the possible hot spot profiles between these two limiting conditions. Furthermore, the superelliptic model can capture changes in gradient inside the hotspot core while using a minimal number of parameters.

A range of hot spot behaviours are explored by varying the exponent of the superellipse. For each exponent a timescale ratio corresponding to an equivalent plateau is determined. Previous work has characterised the influence of this plateau on its surroundings. It is shown that for reference timescale ratios much larger than unity, the plateau and gradient model and the superelliptic model show a similar behaviour. For timescale ratios on the order of unity the gasdynamic response predicted by the plateau and gradient model differs significantly from the more realistic superelliptic model. Slight changes in the superelliptic exponent and reference timescale ratios in the partially confined cases show a high sensitivity to regions of changing temperature gradients throughout the hotspot core. The most significant deviations between the plateau and gradient model and the superelliptic model are observed for timescale ratios between 0.1 and 1. For these smaller timescale ratios, it is found that the temperature profile inside the hot spot core region plays a pivotal role in facilitating detonation formation.

It was shown that the amplitude of the pressure wave created by the hot spot ignition is nearly identical for both the plateau and gradient model and the ellipse. However, the initial emergence of the wave in the plateau/gradient model occurs outside the core region, which causes the reactive media after pressurisation to still be at a low enough temperature that the pressure and reaction waves do not couple. In contrast, in the superelliptic model with the smooth temperature variation inside the core region, the pressure wave emerges inside the core region where the media is at a

sufficiently higher temperature that enables the two waves to couple upon exiting the core region.

Approved for public release: LA-UR-17-28265.

CHAPTER 3. FORMULATION OF CRITICAL TIMESCALES IN HOTSPOT IGNITION

A paper submitted Nov 2017 to *Proceedings of the Combustion Institute* [1]

Fynn Reinbacher [2], Jonathan D. Regele [3,4]

3.1 Abstract

Autoignition of hotspots in thermally stratified reactive mixtures and unreacted fuel-pockets play a significant role in a variety of combustion problems, ranging from HCCI engines to unsteady detonation waves. For a fixed temperature regime, mechanical disturbances created by hotspots and fuel-pockets of finite size have been successfully characterized using acoustic timescale characterization. This work presents an approach to characterize the reaction behavior of both hotspots and fuel-pockets, independent of their thermal stratification, with respect to their surroundings. For this purpose, two dominant timescales in the expansion of a reactive fuel-pocket are identified, given by the minimum required critical expansion speed and the maximal attainable expansion speed for any hotspot or fuel-pocket. The new approach is compared to a hotspot characterization method based on acoustic and excitation timescales. Hotspots and fuel pockets are modeled in a H_2-air mixture using a one-step Arrhenius reaction. It is shown that the new timescale approach predicts the pressure response of both hotspots and fuel-pockets, independent of temperature, in both the hotspot and its surroundings.

[1] *Fynn Reinbacher, Jonathan D. Regele. Formulation of Critical Timescales in Hotspot Ignition.* Proceedings of the Combustion Institute*, (2018)*

[2] Iowa State University Department of Aerospace Engineering

[3] Los Alamos National Laboratory

[4] Author for correspondence: jregele@lanl.gov

3.2 Introduction

Autoignition is a phenomenon associated with localized regions of high reactivity embedded in less or non-reactive surroundings. This behavior occurs in localized hotspots where the temperature is higher than the surroundings as well as unreacted pockets of fuel. Autoignition of a thermally stratified reactive mixture can be readily observed in applications such as HCCI engines, where they form due to various mechanisms such as mechanical friction, wall heat transfer or turbulence [58, 56]. Pockets of unburned fuel have also been observed in unstable cellular detonations, where they form behind the slip line in the shape of a "tongue", which gets pinched off by colliding transverse waves [45, 29].

Hotspots are usually described in terms of linear temperature gradient conditions and characterized by their influence on the transition to detonation [39, 74, 36]. Clarke and Nikiforakis [40] and Clarke [11] have further shown that hotspots can generate compression waves, which facilitate the formation of detonation waves. More recently Kurtz and Regele [31] built on this approach by including a hotspot center of finite size and describing its influence on the surrounding gradient. Reinbacher and Regele [53] further expanded this methodology to smooth temperature variations in the hotspot core region. In both approaches it can be shown that the gas dynamic response strongly depends on the inertial confinement of the hotspot center.

Kassoy [24] performed an asymptotic analysis of the Navier-Stokes equations in which he uses acoustic and heating times to characterize the thermomechanical response of the fluid. The acoustic time t_a is the time it takes for an acoustic wave to propagate a characteristic length l at the local speed of sound a. Varying this heating to acoustic timescale ratio of a local hotspot by two orders of magnitude has been shown to cause a variety of gasdynamic responses, ranging from weak acoustic and compression waves, to strong shock waves [31]. These different types of emitted waves can be traced back to the pressure inside the confined reacting fluid volume, where varying degrees of confinement result in either isobaric, isochoric or mixed reactions, which in turn lead to varying degrees of pressure increase.

Quantifying the pressure response of a hotspot or fuel-pocket based on a reduced set of parameters or measurements could help both predict their influence on the ignition of thermally stratified mixtures and better understand their role in unstable detonations. The aim of this work is to improve the predictability of the pressure response of local reaction hotspots by identifying the dominant timescales and comparing the results to the approach taken in the acoustic timescale analysis. In particular, the influence of the temperature, both inside the hotspot and in the surrounding fluid, will be taken into account.

3.3 Numerical Approach

3.3.1 Mathematical Model

While generally the governing equations for any combustion process are given by the reactive Navier-Stokes equations, in this work the reactive 1-D Euler equations with a one-step Arrhenius reaction will be employed. In the problem at hand the primary focus lies on spontaneous waves and autoignition, which occur on timescales much shorter than those associated with diffusion or viscous effects. Diffusional and viscous transport terms may therefore be neglected. Section 3.4 presents further justification for this approach.

Since the objective of this investigation is the qualitative characterization of the fluids thermomechanical response, one-step kinetics are applied for the chemical model instead of detailed chemistry [22, 6, 59, 37].

The 1-D nondimensional reactive Euler equations are given by

$$\frac{\partial \boldsymbol{U}}{\partial t} + \frac{\partial \boldsymbol{F_x}(\boldsymbol{U})}{\partial x} = \boldsymbol{S} \tag{3.1}$$

with

$$\boldsymbol{U} = \begin{Bmatrix} \rho \\ \rho u \\ \rho e_T \\ \rho Y \end{Bmatrix}, \boldsymbol{F_x} = \begin{Bmatrix} \rho u \\ \rho u^2 + p \\ (\rho e_T + p)u \\ \rho Y u \end{Bmatrix}, \boldsymbol{S} = \begin{Bmatrix} 0 \\ 0 \\ 0 \\ -\dot{W} \end{Bmatrix}, \tag{3.2}$$

the energy equation

$$e_T = \frac{p}{\rho(\gamma - 1)} + \frac{1}{2}u^2 + Yq, \tag{3.3}$$

and the reaction rate

$$\dot{W} = B\rho Y e^{-E_a/T}. \tag{3.4}$$

The Euler equations are nondimensionalized using an arbitrary length l', reference speed of sound $a'_0 = \gamma R T'_0$ and reference temperature $T'_0 = 300K$, such that $T = T'/\gamma T'_0$.

3.3.2 Problem Setup

Under investigation are 4 different hotspot configurations as described by table 3.1. Each Configuration is tested with two different reference lengths L as described in Section 3.4 and for initial hotspot temperatures

$$\boldsymbol{T_4} = \begin{bmatrix} 2 & 3 & 4 & 5 & 10 & 20 & 40 & 80 \end{bmatrix}.$$

The Cases correspond to 1: a fuel pocket in cold inert surroundings, 2: a fuel pocket in burned hot surroundings such that $\boldsymbol{T_4^v} = \boldsymbol{T_4} + q(\gamma - 1)$ the isochoric combustion temperature of the fuel pocket, 3: a fuel pocket in inert hot surroundings, and 4: a hotspot in cold unburned surroundings.

Table 3.1 Initial conditions for 1-D hotspots.

Parameter	Case 1	Case 2	Case 3	Case 4
T_4	$\boldsymbol{T_4}$	$\boldsymbol{T_4}$	$\boldsymbol{T_4}$	$\boldsymbol{T_4}$
T_1	**1**	$\boldsymbol{T_4^v}$	**80**	**1**
Y_4	**1**	**1**	**1**	**1**
Y_1	**0**	**0**	**0**	**1**

In all a cases the initial pressure throughout the domain is $p_4 = p_1 = 1/\gamma$. Table 3.2 lists the reaction parameters for the Arrhenius equation and γ. Figure 3.1 shows the problem set up of the computational domain. The interface at l is smoothed out across a length of $0.05l$ with a hyperbolic tangent, in order to avoid numerical stability issues. Symmetric boundary conditions are used on the left boundary and outflow conditions on the right boundary.

Table 3.2 Arrhenius reaction parameters

Parameter	B	E_a	q	γ
Value	10	17	42	1.2

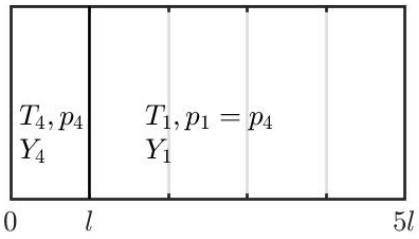

Figure 3.1 Sketch of set up of hotspot in computational domain.

3.3.3 Numerical Method

The parallel adaptive wavelet collocation method (PAWCM) [27, 65] is used to solve the governing equations. A revised hyperbolic solver developed specifically for the PAWCM is used to stabilize shocks and contact discontinuities [48]. In smooth regions the spatial discretization is second order accurate. In regions with shock or contact discontinuities the accuracy reduces to between first and second order. To minimize numerical diffusion and maintain nonlinear stability a van Leer flux limiter is applied [64, 1].

A base grid of 20 grid points is used with 11 levels of refinement, resulting in a maximum of 20,480 effective grid points across the domain. The domain size is based on the initial hotspot size in order to prevent loss and interaction of any flow features across the right boundary. Roughly 4 times this resolution would be required to resolve the von Neumann spike in a steady detonation with an error of less than 1% [31]. Since these simulations are performed during the initial ignition of these hotspots and no steep gradients and discontinuities form during their evolution, the resolution used to perform these simulations is more than adequate.

3.4 Time and Lengthscale Definitions

Mechanical disturbances such as compression or expansion waves travel at the local speed of sound a. For some characteristic length scale l the time required to induce fluid motion is then described by the acoustic time. In the plateau and gradient hotspot model used by Kurtz and Regele [31, 32], the respective lengthscale is that of the roughly isothermal hotspot center. With this approach the acoustic time can be defined:

$$t_a = \frac{l}{a} = \frac{l}{(\gamma R T_4)^{1/2}}. \tag{3.5}$$

Since chemical reactions do not have distinct start and end times, a true excitation time τ_e can not be easily defined. The approach previously used [31, 32] extrapolated the excitation time from the distinct half reaction time τ_r, at which half of the fuel has been consumed. As shown in the schematic in figure 3.2, τ_e is then given by the slope $dY_{0.5}/dt$, obtained from the solution of the Arrhenius equation 3.4. The reaction behavior of a hotspot or fuel pocket of size l can than be characterized by its excitation-to-acoustic timescale ratio:

$$\frac{\tau_e}{t_a} = \frac{\tau_e a}{l} = \frac{L}{l}. \tag{3.6}$$

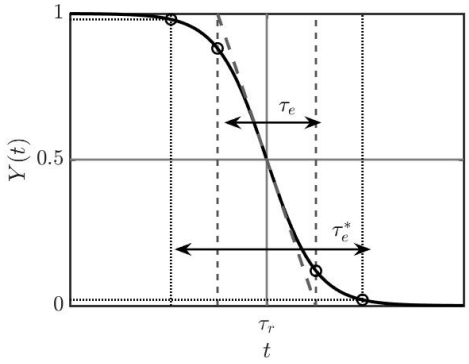

Figure 3.2 Sketch of derivation of excitation times τ_e and τ_e^*. τ_e is defined by linear extrapolation of the fuel consumption at $Y(t) = 0.5$, while τ_e^* is defined by the time frame in which a defined amount of the fuel mass fraction Y is consumed.

Note that both τ_e, a for the model hotspot shown in figure 3.1, and consequently the reference length L are a function of T_4 only. Here L represents the distance an acoustic wave travels inside a hotspot during the excitation time at T_4. The functionality of these two timescales precludes the ability to incorporate effects due to the amount heat released or surrounding temperatures.

The inertial confinement of the reactive volume however is going to depend on the expansion speed of the interface with its surroundings, compared to a critical expansion speed of the hotspot during the given heat release time. From equation 3.3 and the conservation of mass in the hotspot, it can be easily shown that a homogeneous hotspot of given initial length l would need to expand by a length Δl such that

$$\Delta l = \frac{q}{T_4}(\gamma - 1)l, \tag{3.7}$$

in order to maintain constant pressure.

Since the initial pressure in the hotspot and surroundings is the same, the expansion is coupled to the heat release. Thus, the hotspot needs to expand by Δl in the same time interval during which q is released. Using one-step Arrhenius kinetics, the heat release is entirely proportional to the amount of fuel consumed, and the heat release time equivalent to the fuel consumption time. However, the fuel consumption or excitation time τ_e, as defined by the extrapolation from τ_r, and heat release time heat during which almost all fuel is consumed, do not entirely match up. Especially for lower temperatures with longer induction times, a significant amount of heat is released outside the timeframe prescribed by τ_e, which can be easily seen in figure 3.2. We therefore define the full excitation time τ_e^*, as the timeframe during which 99% of the heat is released (99% of fuel is consumed). For comparison, at $T_4 = 2$ the ratio of τ_e^*/τ_e is roughly 5.5, and for $T > 10$, $\tau_e^*/\tau_e \approx 1.5$.

In order to maintain isobaric conditions during the reaction, a hotspot needs to expand by Δl during the heat release time. Based on this information we can therefore define a critical expansion timescale:

$$\tau_{crit} = \tau_e^*. \tag{3.8}$$

Assuming infinitely fast kinetics and thus heat release, we can find the maximum expansion speed of the hotspot by solving the 1-dimensional shock tube [38]:

$$\frac{p_4^v}{p_1} = \frac{p_2}{p_1}\left[1 - \frac{(\gamma-1)(a_1/a_4^v)(p_2/p_1-1)}{(2\gamma)^{1/2}(2\gamma+(\gamma+1)(p_2/p_1-1))^{1/2}}\right]^{-2\gamma/(\gamma-1)}, \tag{3.9}$$

$$u_p = u_2 = a_1\left(\frac{p_2}{p_1}-1\right)\left[\frac{2/\gamma}{(\gamma+1)p_2/p_1+(\gamma-1)}\right]^{1/2}. \tag{3.10}$$

Here p_4^v is the isochoric post-combustion pressure

$$p_4^v = p_4\big(1 + q/T_4(\gamma-1)\big) \tag{3.11}$$

and a_4^v is the speed of sound at the isochoric post-combustion temperature T_4^v given in section 3.3.2. The interface will move at the piston velocity, which is a function of p_2/p_1. This pressure ratio is solved for implicitly through eq. 3.9. From u_p it is clear that the hotspot expansion speed depends on both the initial state inside the hotspot and the heat release (p_4^v, T_4^v) as well as the state of its surroundings (p_1, a_1).

A minimal expansion time for the hotspot can now be formulated, which describes the theoretical minimal time to re-establish isobaric conditions after non-isobaric combustion. This time is given by:

$$t_{exp,min} = \frac{\Delta l}{u_p}. \tag{3.12}$$

Finally, the critical expansion timescale is compared to the minimal expansion time to obtain:

$$\frac{\tau_{crit}}{t_{exp,min}} = \frac{\tau_e^* u_p}{l(\Delta l/l)} = \frac{L^*}{l}. \tag{3.13}$$

The new reference length $L^* = \tau_e^* \cdot u_p/(\Delta l/l)$ represents the maximum distance the hotspot could expand during the excitation time, scaled by the fraction by which the hotspot would need to expand to remain isobaric. In other words, if the critical-to-minimal expansion timescale ratio is small, $\tau_{crit} \ll t_{exp,min}$ ($L^* \ll l$), the hotspot remains inertially confined during the reaction, resulting in a constant volume reaction. If the excitation-to-expansion timescale ratio is large, $\tau_{crit} \gg t_{exp,min}$ ($L^* \gg l$), the hotspot is inertially unconfined and reacts at nearly constant pressure. If the timescale

ratio is $\mathcal{O}(1)$, $\tau_{crit} \approx t_{exp,min}$ ($L^* \approx l$), partial inertial confinement occurs and compression waves are generated.

It should be noted that the viscous and conductive timescales defined by Kassoy [24] $\tau_v = l^2/\nu_0$ and $\tau_c = l^2/\kappa_0$ can be written in terms of the acoustic Reynolds number $Re = l \cdot a_0/\nu_0$ and Prandtl number $Pr = \nu_0/\kappa_0$, such that $\tau_v = Re_a \cdot t_a$ and $\tau_c = Re_a Pr \cdot t_a$. Under the given reference conditions, both are about four orders of magnitude longer than the current timescales of interest and thus are negligible in this context.

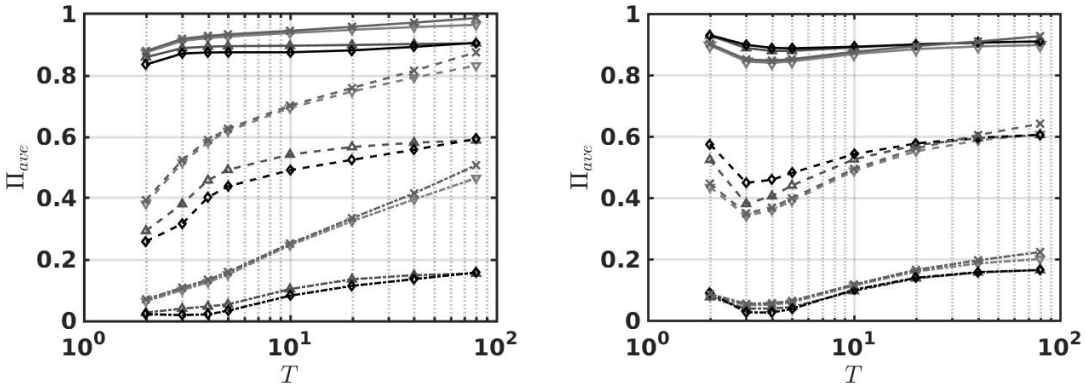

(a) $L = \tau_e \cdot a$ (b) $L^* = \tau_e^* \cdot u_p/(\Delta l/l)$

Figure 3.3 Maximum normalized average pressure in hotspot/fuel-pocket based on reference lengths L and L^* in comparison. (solid) lines for timescale ratios with $l = 10 \cdot L_{ref}$, (dash) lines for timescale ratios with $l = 1 \cdot L_{ref}$, (dot-dash) lines for timescale ratios with $l = 0.1 \cdot L_{ref}$. $\bigtriangledown$: Case 1, $\diamond$: Case 2, $\bigtriangleup$: Case 3, $\times$: Case 4, as described in table 3.1.

3.5 Results

In order to understand the difference in behavior between these two characterization approaches, it is convenient to look at the pressure rise inside the hotspot throughout the reaction. The initial reaction time for this purpose is is assumed to last from $t_0 = 0$, at the beginning of the simulation, until t_{end} when the average fuel mass fraction inside the hotspot has dropped to $Y = 0.01$, or 99% of the fuel has been consumed.

Figure 3.3 shows the average normalized pressure inside the original hotspot from $x = 0$ to $x = l$ after the combustion has completed. The normalized pressure Π for this purpose is given by

$$\Pi = \frac{p - p_4}{p_4^v - p_4} \tag{3.14}$$

where p is the pressure inside the hotspot, p_4 is the initial pressure and p_4^v the isochoric pressure as given by equation 3.11. A pressure of $\Pi = 1$ indicates a perfectly isochoric reaction and a pressure of $\Pi = 0$ indicates perfectly isobaric.

In fig 3.3(a) the results for the model cases based on the acoustic timescale characterization are presented, while fig 3.3(b) shows the results based on the new expansion timescale approach. For timescale ratios much larger than unity ($l = 10 \cdot L_{ref}$, solid lines) it can be seen that both models predict almost perfectly isochoric conditions. The acoustic timescale characterization yields average maximum pressures between $\Pi = 0.8$, in Case 2 ($\diamond$) for an initial fuel-pocket temperature of $T = 2$ surrounded by hot burned gas, and $\Pi \approx 1$, in Case 4 for a hotspot at an initial temperature of $T = 80$ surrounded by cold unreacted gas.

In general the maximum pressure increases with both, initial hotspot/fuel-pocket temperature and decreasing temperature in the surrounding gas. Arbitrarily hot ambient gas in Case 3 ($\triangle$) at $T = 80$ leads to slightly higher pressures than ambient gas at T^v in Case 2 ($\diamond$). This effect diminishes as the relative temperature difference between surroundings and fuel-pocket decreases for increasing T. For fuel-pockets and hotspots in initially cold surroundings (Cases 1 and 4, $\bigtriangledown$ and $\times$) the maximum pressure becomes higher, relative to those in hot surroundings and increases with initial temperature and thus temperature difference to its surroundings. Unreacted fuel in the cold surroundings increases the final pressure at high initial temperatures.

Two factors increase the final average pressure resulting from the reaction and thus confinement, for constant acoustic timescale ratios: growing temperature differences between hotspot/fuel-pocket and its surroundings, and higher initial temperatures. This becomes even more apparent when the acoustic timescale ratio of the hotspot is on the order of, or smaller than unity. For an acoustic timescale ratio of 1 (figure 3.3(a), dash) the fuel-pockets in hot surroundings (Cases 2 and 3) reach average pressures of Π between 0.25 and 0.6, while fuel-pocket and hotspot in cold surroundings (Cases 1 and 4) reach average pressures of Π between 0.4 and almost 0.9. This means that despite an acoustic timescale ratio of unity, which would predict mixed isochoric and isobaric behavior, extremely hot initial temperatures in cold surroundings react nearly isochorically.

Similarly for initial acoustic timescale ratios an order of magnitude smaller than unity (figure 3.3(a), dot-dash), which predict an isobaric reaction, at high initial temperatures ($T > 7$) the average pressure exceeds $\Pi = 0.2$ and reaches up to 0.5, resulting in mixed isobaric and isochoric

reactions. Just like in the partially confined cases (dash) and strongly confined cases (solid), the maximum pressures increase for higher initial hotspot temperatures, in cold surroundings and in the presence of additional fuel in the surroundings.

Figure 3.3(b) shows the same results for hotspots and fuel-pockets characterized based on their critical expansion timescales. For timescale ratios an order of magnitude larger than unity (solid) the maximum pressure Π ranges from 0.85 to 0.95 across all cases. The variance of maximum pressure Π remains in a range of $\Delta\Pi \approx 0.05$ for every initial temperature, independent of the conditions in the surrounding fluid. All cases can be considered to be react almost isochorically.

With critical expansion timescale ratios on the order of unity, the average maximum pressures Π range from roughly 0.35 to 0.6 (figure 3.3(b), dash). Independent of the temperature in the surrounding fluid the variance of Π for each initial temperature lies within $\Delta\Pi \approx 0.2$ and decreases with increasing T. For temperatures $T > 6$ all Π lie within 0.1. At temperatures above 20 it is almost 0 with the exception of the hotspot (Case 4, $\times$). All Cases can be considered to be mixed isochoric and isobaric reactions.

In the unconfined cases (figure 3.3(b), dot-dash) all Π lie between 0.02 and 0.22, yielding nearly isobaric reactions. The variation in Π between cases at each initial temperature lies in a range of $\Delta\Pi \approx 0.05$. For initial temperatures above 5 all Π start to increase and exceed 0.1 starting at $T \approx 10$.

3.6 Discussion

Fuel-pockets and hotspots have been characterized based on an acoustic-to-excitation and critical expansion timescale ratio in order to make a-priori predictions on the reaction mode of the fluid volume. Based on the maximum pressure increase of the average pressure during the reaction, the reaction was described as either isochoric, isobaric or mixed type. Cold ambient fluid surrounding the local reaction hotspot has been shown to increase the inertial confinement, resulting in more isochoric reactions in hotspots characterized based on an acoustic-to-excitation timescale.

This effect can be accounted for by using the critical expansion timescale ratio as a reference for hotspot description. Even for temperatures in the surrounding fluid varying by almost two orders of magnitude, the expected reaction behaviour (isochoric, isobaric, mixed) still matches that predicted based on the timescale ratio. The variation in the resulting normalized pressure in cases expected to react in a similar fashion for the same initial temperature, could be reduced to less than 5% for isochoric and isobaric cases, and about (20%) in mixed cases. However the variation in average expected pressure for the same timescale ratio still varies significantly with increasing initial hotspot/fuel-pocket temperature.

With a dimensional reference temperature of $T_0' = 300K$ and a non-dimensionalization $T = T'/(\gamma T_0')$, reactions at initial temperature of $T > 10$ (here $T' = 3600K$) become almost irrelevant for any real combustion systems involving complex chemistry. Under these conditions predictions made by the acoustic-to-excitation and critical-expansion timescale characterization become more similar. Nonetheless, reducing the temperature range in question does not alleviate the discrepancies in the predictions made by the acoustic timescale-to-exciation timescale characterization for fuel pockets in hot surroundings and fuel-pockets/hotspots in cold surroundings.

In the high temperature limit the Arrhenius reaction rate becomes temperature independent. Under these conditions, the induction time and any fuel consumption and heat release during this phase, become negligible. For technically relevant temperature ranges on the other hand, the induction time and variation in heat release can be expected to play significant roles. Complex chemistry would most likely change slow chemistry and heat release during the induction time. The current approach to define the critical expansion time essentially considers all heat to be released at a constant rate during both slow and fast heat release. Weighing the critical expansion rates during fast and slow heat release periods might be necessary to improve the method, especially for complex chemistry.

3.7 Conclusion

A new characterization method based on critical expansion timescales has been successfully used to predict the reaction mode of hotspots and fuel-pockets. In comparison to a previously employed characterization method based on acoustic and excitation timescales, the new approach offers significant improvement in the prediction of the pressure increase in local reactive fluid volume during autoignition, independent of temperature in the local reaction hotspot and its surroundings. This may allow more accurate predictions of the overall thermomechanical response of the surrounding fluid, as well as predict the type and strength of emitted acoustic, compression or shock waves. Future studies should investigate the influence of complex chemistry and multiple dimensions with respect to the new method.

Approved for public release: LA-UR-17-30824.

CHAPTER 4. CONCLUSIONS

Hotspots are modeled using a superelliptic model for smooth temperature variations at a local hotspot center of finite size, in combination with a linear temperature gradient. With the superelliptic model, temperature distributions taking the shape of the well studied gradient only, and plateau-gradient hotspot types could be modeled, as well all possible profiles in between these limiting cases. With the superelliptic model, hotspot cores of various sizes were explored and compared to results obtained by equivalent plateau-gradient type hotspots, with plateau lengths corresponding to timescale ratios spanning two order of magnitude. For reference timescale ratios smaller than unity, for which the hotspot core regions are expected to react mostly or fully isochorically, changes in smooth temperature variation turned out to play a pivotal role in direct detonation initiation. While the amplitude of the compression wave emitted by a hotspot-core of the same reference timescale ratio is almost identical for plateau and elliptic core, the location of its emergence is not. In the ellipse type hotspots it emerges inside the hotspot core, whereas in plateau type hotspots it first appears outside the core region. This changes the initial temperature of the subsequently pressurized gas. Without sufficiently high enough initial temperature, the pressure wave and reaction reaction wave are not able to couple and facilitate transition to detonation.

Additionally a new timescale characterization method was developed and tested. Similar to the acoustic timescale characterization, it derives one required expansion timescale from the isochoric excitation time or the reactive medium, the time during which heat is released in the fluid. A critical expansion timescale is derived based on the maximum possible expansion speed and the required expansion length to reestablish isobaric conditions, of a fluid volume to which energy is added instantaneously. Since this critical expansion time, unlike the acoustic time, is dependent on the conditions both inside the reactive hotspot and its surrounding, this new method was able to make more accurate predictions over a wider range of conditions for hotspots, unburned fuel

pockets and fuel bubbles. For a known reactive mixture, this method can help to gauge the impact of a reacting hotspot in situations the pressure release can otherwise not be measured or resolved.

Future studies should investigate the influence of detailed kinetics in contrast to the 1-step Arrhenius mechanism used here. Acoustic timescale characterization type methods seek to successfully normalize the hotspot reaction behavior in terms of the heat release or excitation time scales. Results such as those obtained by Sharpe and Shorte [59] and Liberman et al. [37] have shown the impact of kinetics on the reaction in temperature gradients, where the gas dynamic response is mostly dependent on the induction time scales. The effect kinects the reaction timescales during hotspot driven direct detonation initiation would be extremely interesting to investigate. Further an extension in to multiple dimensions similar to Kurtz and Regele [32] should be made. Significant effects on the critical expansion timescale as obtained in chapter 3.7 can be expected, as for spherical hotspots minimal expansion lengths translate into expansion areas in 2D, and expansion volumes in 3D.

BIBLIOGRAPHY

[1] Anderson, W. K., Thomas, J. L., and Van Leer, B. (1986). Comparison of finite volume flux vector splittings for the euler equations. *AIAA journal*, 24(9):1453–1460.

[2] Antunes, J. G., Mikalsen, R., and Roskilly, A. (2008). An investigation of hydrogen-fuelled hcci engine performance and operation. *International Journal of Hydrogen Energy*, 33(20):5823–5828.

[3] Bach, G., Knystautas, R., and Lee, J. (1971). Initiation criteria for diverging gaseous detonations. In *Symposium (International) on Combustion*, volume 13, pages 1097–1110. Elsevier.

[4] Bane, S. P. M. (2010). *Spark ignition: experimental and numerical investigation with application to aviation safety*. PhD thesis, California Institute of Technology.

[5] Bhagatwala, A., Sankaran, R., Kokjohn, S., and Chen, J. H. (2015). Numerical investigation of spontaneous flame propagation under rcci conditions. *Combustion and Flame*, 162(9):3412–3426.

[6] Bradley, D. and Kalghatgi, G. (2009). Influence of autoignition delay time characteristics of different fuels on pressure waves and knock in reciprocating engines. *Combustion and flame*, 156(12):2307–2318.

[7] Chapman, D. L. (1899). Vi. on the rate of explosion in gases. *The London, Edinburgh, and Dublin Philosophical Magazine and Journal of Science*, 47(284):90–104.

[8] Chen, J. H., Hawkes, E. R., Sankaran, R., Mason, S. D., and Im, H. G. (2006). Direct numerical simulation of ignition front propagation in a constant volume with temperature inhomogeneities: I. fundamental analysis and diagnostics. *Combustion and flame*, 145(1-2):128–144.

[9] Chi, C., Abdelsamie, A., and Thévenin, D. (2018). Direct numerical simulations of hotspot-induced ignition in homogeneous hydrogen-air pre-mixtures and ignition spot tracking. *Flow, Turbulence and Combustion*, pages 1–19.

[10] Christensen, M., Hultqvist, A., and Johansson, B. (1999). Demonstrating the multi fuel capability of a homogeneous charge compression ignition engine with variable compression ratio. Technical report, SAE Technical Paper.

[11] Clarke, J. (1989). Fast flames, waves and detonation. *Progress in energy and combustion science*, 15(3):241–271.

[12] Clarke, J., Kassoy, D., and Riley, N. (1984a). Shocks generated in a confined gas due to rapid heat addition at the boundary. i. weak shock waves. In *Proc. R. Soc. Lond. A*, volume 393, pages 309–329. The Royal Society.

[13] Clarke, J., Kassoy, D., and Riley, N. (1984b). Shocks generated in a confined gas due to rapid heat addition at the boundary. ii. strong shock waves. In *Proc. R. Soc. Lond. A*, volume 393, pages 331–351. The Royal Society.

[14] Clarke, J., Kassoy, D., and Riley, N. (1986). On the direct initiation of a plane detonation wave. *Proc. R. Soc. Lond. A*, 408(1834):129–148.

[15] Döring, W. (1943). Über den detonationsvorgang in gasen. *Annalen der Physik*, 435(6-7):421–436.

[16] Edwards, D., Hooper, G., Morgan, J., and Thomas, G. (1978). The quasi-steady regime in critically initiated detonation waves. *Journal of Physics D: Applied Physics*, 11(15):2103.

[17] Gu, X., Emerson, D., and Bradley, D. (2003). Modes of reaction front propagation from hot spots. *Combustion and flame*, 133(1-2):63–74.

[18] Jaasim, M., Hernandez Perez, F., Vedharaj, S., Vallinayagam, R., Dibble, R. W., and Im, H. G. (2017). Effect of timing and location of hotspot on super knock during pre-ignition. *SAE Technical Paper Series*.

[19] Jackson, T., Kapila, A., and Stewart, D. (1989). Evolution of a reaction center in an explosive material. *SIAM Journal on Applied Mathematics*, 49(2):432–458.

[20] Jouguet, E. (1905). Sur la propagation des réactions chimiques dans les gaz. *J. Maths. Pure Appl.*, 7:347.

[21] Kaiser, S., Schild, M., and Schulz, C. (2013). Thermal stratification in an internal combustion engine due to wall heat transfer measured by laser-induced fluorescence. *Proceedings of the combustion institute*, 34(2):2911–2919.

[22] Kalghatgi, G. T. and Bradley, D. (2012). Pre-ignition and super-knockin turbo-charged spark-ignition engines. *International Journal of Engine Research*, 13(4):399–414.

[23] Kapila, A., Schwendeman, D., Quirk, J., and Hawa, T. (2002). Mechanisms of detonation formation due to a temperature gradient. *Combustion Theory and Modelling*, 6(4):553–594.

[24] Kassoy, D. (2010). The response of a compressible gas to extremely rapid transient, spatially resolved energy addition: an asymptotic formulation. *Journal of Engineering Mathematics*, 68(3):249–262.

[25] Kassoy, D. (2014). Non-diffusive ignition of a gaseous reactive mixture following time-resolved, spatially distributed energy deposition. *Combustion Theory and Modelling*, 18(1):101–116.

[26] Kassoy, D. R., Kuehn, J. A., Nabity, M., and Clarke, J. (2008). Detonation initiation on the microsecond time scale: Ddts. *Combustion Theory and Modelling*, 12(6):1009–1047.

[27] Kevlahan, N. K. and Vasilyev, O. V. (2005). An adaptive wavelet collocation method for fluid-structure interaction at high reynolds numbers. *SIAM Journal on Scientific Computing*, 26(6):1894–1915.

[28] Khokhlov, A. M. and Oran, E. S. (1999). Numerical simulation of detonation initiation in a flame brush: the role of hot spots. *Combustion and Flame*, 119(4):400–416.

[29] Kiyanda, C. and Higgins, A. (2013). Photographic investigation into the mechanism of combustion in irregular detonation waves. *Shock Waves*, 23(2):115–130.

[30] Knystautas, R. and Lee, J. (1976). On the effective energy for direct initiation of gaseous detonations. *Combustion and flame*, 27:221–228.

[31] Kurtz, M. D. and Regele, J. D. (2014a). Acoustic timescale characterisation of a one-dimensional model hot spot. *Combustion Theory and Modelling*, 18(4-5):532–551.

[32] Kurtz, M. D. and Regele, J. D. (2014b). Acoustic timescale characterisation of symmetric and asymmetric multidimensional hot spots. *Combustion Theory and Modelling*, 18(6):711–729.

[33] Lee, J. (2008). *The Detonation Phenomenon*. Cambridge University Press.

[34] Lee, J., Knystautas, R., and Yoshikawa, N. (1978). Photochemical initiation of gaseous detonations. In *Gasdynamics of Explosions and Reactive Systems*, pages 971–982. Elsevier.

[35] Lee, J. and Moen, I. (1980). The mechans of transition from deflagration to detonation in vapor cloud explosions. *Progress in Energy and Combustion Science*, 6(4):359–389.

[36] Lee, J. H. (1977). Initiation of gaseous detonation. *Annual Review of Physical Chemistry*, 28(1):75–104.

[37] Liberman, M., Kiverin, A., and Ivanov, M. (2011). On detonation initiation by a temperature gradient for a detailed chemical reaction models. *Physics Letters A*, 375(17):1803–1808.

[38] Liepmann, H. W. and Roshko, A. (1957). *Elements of gasdynamics*. Courier Corporation.

[39] Merzhanov, A. (1966). On critical conditions for thermal explosion of a hot spot. *Combustion and Flame*, 10(4):341–348.

[40] Nikiforakis, N. and Clarke, J. F. (1996). Quasi-steady structures in the two-dimensional initiation of detonations. In *Proc. R. Soc. Lond. A*, volume 452, pages 2023–2042. The Royal Society.

[41] Oppenheim, A. K. (2014). *Introduction to Gasdynamics of Explosions: Course Held at the Department of Hydro-and Gas-Dynamics, September 1970*, volume 48. Springer.

[42] Oran, E. S. and Khokhlov, A. M. (1999). Deflagrations, hot spots, and the transition to detonation. *Philosophical Transactions of the Royal Society of London A: Mathematical, Physical and Engineering Sciences*, 357(1764):3539–3551.

[43] Poland, J. and Kassoy, D. (1983). The induction period of a thermal explosion in a gas between infinite parallel plates. *Combustion and Flame*, 50:259–274.

[44] Radhwan, A. and Kassoy, D. (1984). The response of a confined gas to a thermal disturbance: rapid boundary heating. *Journal of engineering mathematics*, 18(2):133–156.

[45] Radulescu, M. I., Sharpe, G. J., Law, C. K., and Lee, J. H. (2007). The hydrodynamic structure of unstable cellular detonations. *Journal of Fluid Mechanics*, 580:31–81.

[46] Regele, J., Kassoy, D., and Vasilyev, O. (2012). Effects of high activation energies on acoustic timescale detonation initiation. *Combustion Theory and Modelling*, 16(4):650–678.

[47] Regele, J., Kassoy, D., and Vasilyev, O. (2013a). Purely gasdynamic multidimensional indirect detonation initiation using localized acoustic timescale power deposition. In *51st AIAA Aerospace Sciences Meeting including the New Horizons Forum and Aerospace Exposition*, page 1172.

[48] Regele, J. and Vasilyev, O. (2009). An adaptive wavelet-collocation method for shock computations. *International Journal of Computational Fluid Dynamics*, 23(7):503–518.

[49] Regele, J. D. (2013). Effects of inertial confinement on the ignition of diffusion-free unreacted pockets. In *24th International Colloquium on the Dynamics of Explosions and Reactive Systems (ICDERS), Taipei Taiwan*, volume 28, pages 1–6.

[50] Regele, J. D. (2015). Acoustic timescale characterization of unreacted pockets in unstable detonation waves. In *25th International Colloquium on the Dynamics of Explosions and Reactive Systems (ICDERS), Leeds UK*.

[51] Regele, J. D., Kassoy, D. R., Aslani, M., and Vasilyev, O. V. (2016). Evolution of detonation formation initiated by a spatially distributed, transient energy source. *Journal of Fluid Mechanics*, 802:305–332.

[52] Regele, J. D., Kassoy, D. R., Vezolainen, A., and Vasilyev, O. V. (2013b). Indirect detonation initiation using acoustic timescale thermal power deposition. *Physics of Fluids*, 25(9):091113.

[53] Reinbacher, F. and Regele, J. D. (2018). Influence of smooth temperature variation on hotspot ignition. *Combustion Theory and Modelling*, 22(1):110–130.

[54] Sankaran, R., Im, H. G., Hawkes, E. R., and Chen, J. H. (2005). The effects of non-uniform temperature distribution on the ignition of a lean homogeneous hydrogen–air mixture. *Proceedings of the Combustion Institute*, 30(1):875–882.

[55] Schmitt, M. (2014). *Direct numerical simulations in engine-like geometries*. PhD thesis, ETH Zurich.

[56] Schmitt, M., Frouzakis, C. E., Wright, Y. M., Tomboulides, A. G., and Boulouchos, K. (2016). Investigation of wall heat transfer and thermal stratification under engine-relevant conditions using dns. *International Journal of Engine Research*, 17(1):63–75.

[57] Semerok, A., Chaléard, C., Detalle, V., Lacour, J.-L., Mauchien, P., Meynadier, P., Nouvellon, C., Sallé, B., Palianov, P., Perdrix, M., et al. (1999). Experimental investigations of laser ablation efficiency of pure metals with femto, pico and nanosecond pulses. *Applied Surface Science*, 138:311–314.

[58] Shah, A., Brindley, J., McIntosh, A., and Griffiths, J. (2007). Ignition and combustion of low-exothermicity porous materials by a local hotspot. In *Proceedings of the Royal Society of London A: Mathematical, Physical and Engineering Sciences*, volume 463, pages 1287–1305. The Royal Society.

[59] Sharpe, G. J. and Short, M. (2003). Detonation ignition from a temperature gradient for a two-step chain-branching kinetics model. *Journal of Fluid Mechanics*, 476:267–292.

[60] Sileem, A., Kassoy, D., and Hayashi, A. (1991). Thermally initiated detonation through deflagration to detonation transition. *Proc. R. Soc. Lond. A*, 435(1895):459–482.

[61] Strehlow, R. (1968). Fundamentals of combustion. *Int Textbook Company, Scranton, PA*, pages 287–290.

[62] Thomas, P. (1973). An approximate theory of hot spot critically. *Combustion and Flame*, 21(1):99–109.

[63] Urtiew, P. and Oppenheim, A. (1966). Experimental observations of the transition to detonation in an explosive gas. *Proc. R. Soc. Lond. A*, 295(1440):13–28.

[64] Van Leer, B. (1982). Flux-vector splitting for the euler equations. In *Eighth international conference on numerical methods in fluid dynamics*, pages 507–512. Springer.

[65] Vasilyev, O. V. and Bowman, C. (2000). Second-generation wavelet collocation method for the solution of partial differential equations. *Journal of Computational Physics*, 165(2):660–693.

[66] Von Neumann, J. (1942). Theory of detonation waves. office of scientific research and development. *National Defense Research Committee Div. B. Technical Report*, 549.

[67] Wang, Z., Qi, Y., He, X., Wang, J., Shuai, S., and Law, C. K. (2015). Analysis of pre-ignition to super-knock: hotspot-induced deflagration to detonation. *Fuel*, 144:222–227.

[68] Wei, H., Chen, C., Shu, G., Liang, X., and Zhou, L. (2018). Pressure wave evolution during two hotspots autoignition within end-gas region under internal combustion engine-relevant conditions. *Combustion and Flame*, 189:142–154.

[69] Yang, C. (1962). Theory of ignition and auto-ignition. *Combustion and Flame*, 6:215–225.

[70] Zaturska, M. B. (1975). Thermal explosion of interacting hot spots. *Combustion and Flame*, 25:25–30.

[71] Zeldovich, J. (1942). Theory of nucleation and condensation. *Soviet Physics–JETP (English Translation)*, 12:525.

[72] Zeldovich, Y. B. (1940). On the theory of detonation propagation in gaseous systems. *Zh. Eksp. Teor. Fiz*, 10(5):542–568.

[73] Zeldovich, Y. B. (1980). Regime classification of an exothermic reaction with nonuniform initial conditions. *Combustion and Flame*, 39(2):211–214.

[74] Zel'Dovich, Y. B., Librovich, V., Makhviladze, G., and Sivashinskil, G. (1970). On the onset of detonation in a nonuniformly heated gas. *Journal of Applied Mechanics and Technical Physics*, 11(2):264–270.

[75] Zhang, B., Ng, H. D., and Lee, J. H. (2012). Measurement and scaling analysis of critical energy for direct initiation of gaseous detonations. *Shock Waves*, 22(3):275–279.